The pulse: transient fMRI signal increases in subcortical arousal systems during transitions in attention

Rong Li[a,d], **Jun Hwan Ryu**[a], **Peter Vincent**[a], **Max Springer**[a], **Dan Kluger**[a], **Erik A. Levinsohn**[a], **Yu Chen**[a], **Huafu Chen**[d], **Hal Blumenfeld**[a,b,c,*]

[a]Departments of Neurology, Yale University School of Medicine, 333 Cedar Street, New Haven, CT 06520, United States

[b]Departments of Neuroscience, Yale University School of Medicine, 333 Cedar Street, New Haven, CT 06520, United States

[c]Departments of Neurosurgery, Yale University School of Medicine, 333 Cedar Street, New Haven, CT 06520, United States

[d]MOE Key Lab for Neuroinformation, High-Field Magnetic Resonance Brain Imaging Key Laboratory of Sichuan Province, School of Life Science and Technology, University of Electronic Science and Technology of China, Chengdu 610054, P R China

Abstract

Studies of attention emphasize cortical circuits for salience monitoring and top-down control. However, subcortical arousal systems have a major influence on dynamic cortical state. We hypothesize that task-related increases in attention begin with a "pulse" in subcortical arousal and cortical attention networks, which are reflected indirectly through transient fMRI signals. We conducted general linear model and model-free analyses of fMRI data from two cohorts and tasks with mixed block and event-related design. 46 adolescent subjects at our center and 362 normal adults from the Human Connectome Project participated. We identified a core shared network of transient fMRI increases in subcortical arousal and cortical salience/attention networks across cohorts and tasks. Specifically, we observed a transient pulse of fMRI increases both at task block onset and with individua task events in subcortical arousal areas including midbrain tegmentum, thalamus, nucleus basalis and striatum; cortical-subcortical salience network regions including the anterior insula/claustrum and anterior cingulate cortex/supplementary motor area; in dorsal attention network regions including dorsolateral frontal cortex and inferior parietal lobule; as well as in motor regions including cerebellum, and left hemisphere hand primary motor cortex. The transient pulse of fMRI increases in subcortical and cortical arousal and attention networks was consistent across tasks and study populations, whereas sustained activity in these same networks

was more variable. The function of the transient pulse in these networks is unknown. However, given its anatomical distribution, it could participate in a neuromodulatory surge of activity in multiple parallel neurotransmitter systems facilitating dynamic changes in conscious attention.

Keywords

Attention; fMRI; Midbrain; Thalamus; Consciousness; Arousal

1. Introduction

Sustained changes in attention, arousal and consciousness are known to be under modulatory control of subcortical arousal systems. The thalamus, upper brainstem, basal forebrain and striatum play key roles in such temporally extended states as sustained attention, sleep-wake regulation and in chronic disorders of consciousness (Laureys et al., 2015; Posner et al., 2007; Steriade and McCarley, 2010). However, the possible role of these same subcortical arousal systems in transient and dynamic moment-to-moment modulation of attention has been less thoroughly investigated (Sarter and Lustig, 2019; Schiff et al., 2013). Most work on dynamic changes in attention instead focuses on well-characterized cortical systems involved in stimulus salience and top-down attentional control (Corbetta and Shulman, 2002a; Seeley et al., 2007). Our goal was to determine whether subcortical systems typically implicated in static states of arousal and attention may dynamically participate through a transient pulse of increased activity at the onset of changes in attention.

The blood-oxygenation level-dependent (BOLD) response measured by functional magnetic resonance imaging (fMRI) has been used extensively in mixed block and event-related task designs, enabling independent detection of transient and sustained BOLD responses (Buckner et al., 1996; Dosenbach et al., 2007; Fox et al., 2005c; Shulman et al., 1997; Visscher et al., 2003). Cortical BOLD fMRI signal increases (or more simply "fMRI increases") at onset and offset of blocks and events have been observed in widely distributed networks (Fox et al., 2005a; Paret et al., 2014; Uludag, 2008). These findings highlight the need for an increased understanding of both cortical and subcortical BOLD responses at block transitions and with target event stimuli.

Subcortical structures including the midbrain reticular formation, intralaminar thalamic nuclei and striatum have long been implicated in information processing related to adjustments of arousal and maintenance of attentive states (Faingold and Blumenfeld, 2013; Kinomura et al., 1996; Schiff and Plum, 2000b; Van der Werf et al., 2002). Previous studies have also indicated a specific role for the midbrain and intralaminar thalamus (Kinomura et al., 1996; Portas et al., 1998), as well as the basal forebrain and nucleus basalis in cortical arousal and attention (Fuller et al., 2011; Raver and Lin, 2015). However, the neural substrates of transient changes in attention particularly in subcortical structures, and the dynamic time course of these changes which may be crucial for driving neural systems between attention states have not been fully investigated in human subjects.

In this study, we seek to systematically investigate the involvement of subcortical arousal systems and cortical networks in transient changes in attention using both block and event-

related fMRI designs across different populations and task paradigms. First, we conducted a general linear model-based analysis to identify neural networks for transient and sustained fMRI changes across task paradigms and study populations. Recent studies illustrate that model-free fMRI analyses can provide important information on functional localization (Cauda et al., 2014; Gonzalez-Castillo et al., 2012; Guo et al., 2016). To that end, we performed a model-free voxel-based analysis of fMRI percent signal changes for the whole brain using massive averaging to examine the dynamic brain responses during the onset of attention-demanding behavioral task blocks. Next, we examined mean fMRI time courses in specific anatomical cortical and subcortical regions. We performed a final conjunction analysis revealing a common network of cortical and subcortical areas activated with task block onset, as well as with individual task trials. This approach allowed us to systematically characterize a transient pulse of fMRI increases in a common network of subcortical arousal systems, as well as in cortical salience and attention systems, which may provide new insights into brain mechanisms of arousal and attention.

2. Materials and methods

2.1. Subjects

The current study is based on two different datasets. A summary listing of subject demographics, task conditions, and scanning parameters is given in Table 1. For the first dataset we used subjects from our previously reported study of attention impairment in childhood absence epilepsy (Bai et al., 2011; Guo et al., 2016; Killory et al., 2011). Our current analysis of this dataset included a total of 46 subjects, consisting of both healthy normal adolescents ($n = 22$) and adolescents with childhood absence epilepsy ($n = 24$), 26 males and 20 females, with a mean age of 13 years (range 11–19 years). The purpose of including both normal subjects and subjects with absence epilepsy was to increase the sample size of the cohort. However, we implemented several procedures to ensure the results of this analyses were not skewed by abnormal activity in the absence subgroup. Inclusion and exclusion criteria for the subjects with absence epilepsy were described previously and included electroencephalography (EEG) showing a normal background outside the absence episodes; and no structural brain abnormalities or other neurological disorders (Bai et al., 2010; Guo et al., 2016). For the absence epilepsy subjects we excluded any data runs containing epileptiform activity based on simultaneously acquired EEG-fMRI (Bai et al., 2011, 2010; Guo et al., 2016; Killory et al., 2011). In addition, all analyses were first performed separately on the normal and absence epilepsy adolescents to ensure the results were similar before combining data across these groups (results from healthy normal adolescents alone and epilepsy alone are shown in Supplementary Figures for comparison). All human procedures were approved by the Yale University Institutional Review Board, and all subjects provided written informed assent and parental consent.

The second dataset was selected from a large sample of task-fMRI data publicly released through the Human Connectome Project (HCP) 900 Subjects Data Release (Barch et al., 2013; Hodge et al., 2016; Van Essen et al., 2013) (http://humanconnectome.org). We analyzed data from the HCP gambling task (Delgado et al., 2000) because this consisted of a block-design behavioral task with no distinct task onset cue stimulus at the beginning of

each block. The HCP gambling task dataset includes 362 subjects, 359 young healthy adults from 22 to 35 years old and 3 healthy adults older than 36 (186 females). The use of HCP data in this study was also approved by the Yale University Institutional Review Board.

2.2. Behavioral tasks

Two behavioral tasks were performed during the fMRI acquisitions for each Yale adolescent subject. These behavioral tasks have been used previously (Bai et al., 2010; Guo et al., 2016; Killory et al., 2011; Mirsky and Vanburen, 1965) to examine attentional vigilance. Both tasks were generated using E-Prime 1.1 (Psychology Software Tools, Inc. Pittsburgh, PA). Each task run consisted of alternating blocks of fixation and task, with fixation blocks lasting 32 s and task blocks lasting either 32 s or 96 s (Table 1, Supplementary Figure 1A, B). Total behavioral run duration was 640 s and fMRI run duration slightly longer at 644.8 s. Each run contained of only one type of behavioral task—either the continuous performance task (CPT) or the repetitive tapping task (RTT). Up to 6 data runs (typically 3 or 4) were obtained per subject as tolerated within a 1–1.5 hour scanner session. During the CPT, 16 letters were displayed for 250 ms each in a randomized sequence (e.g. A B C D E F H I L M N O T X Y Z). Twenty-five percent of all letters shown were the target X, and subjects were instructed to respond to the target letter X by using their right thumb to push a button. The RTT required the subjects to push the button with their right thumb for every displayed letter and no letter X appeared in the sequence. For both tasks, white letters or a luminance-matched fixation cross appeared on a black background, using a rear-projection screen viewed by a mirror mounted on the patient head coil. The E-Prime program was used to record both the stimuli and button push response times for displayed letters (see Supplementary Figure 1A and 1B for additional details of the CPT/RTT task).

The HCP gambling task was adapted from a version developed by Delgado and colleagues (Barch et al., 2013; Delgado et al., 2000; May et al., 2004; Tricomi et al., 2004); see also Reference Manual of HCP 900 Subjects Data Release on Page 42–43: (https://www.humanconnectome.org/storage/app/media/documentation/s900/HCP_S900_Release_Reference_Manual.pdf). In the task, the subjects played a card guessing game, in which they were asked to guess the number on a mystery card (represented by a "?") in order to win or lose money (Supplementary Figure 1C). The subjects were told that the card numbers range from 1–9, and were asked to guess whether the number was more or less than 5 by pressing one of the two buttons on the response box using their right hands. At the onset of each trial, the "?" mystery card was presented for up to 1500 ms (if the participant responded before the time, a fixation cross was displayed for the remaining time), followed by a feedback period of 1000 ms which showed the number on the mystery card. The feedback also included either 1) a green upward arrow with "$1" for reward trials, 2) a red downward arrow next to -$0.50 for loss trials, or 3) the number 5 and a gray double-headed horizontal arrow for neutral trials. Then, there was a 1000 ms inter-trial interval with a fixation cross presented on the screen. Of note, this sequence resulted in a total period of exactly 3.5 s between onset of consecutive trials within a block. The task was presented in blocks of 8 trials, for a total of ~28 s per task block. In each run, there was an initial 8 s countdown sequence of numbers displayed before the first task block, followed by 2 mostly reward and 2 mostly loss blocks, interleaved with 4 fixation blocks

(~15 s each). Total fMRI run duration was 192 s, or slightly longer than the behavioral run duration. Two runs were obtained per subject. Of note, unlike the CPT and RTT tasks, the fixation and task periods in the gambling task were not luminance matched. Fixation periods in the gambling task consisted of a white cross on a black background, whereas task periods consisted of a combination of white letters and colored arrows on a black background (see Supplementary Figure 1C for additional details of the gambling task).

2.3. fMRI data acquisition

All Yale adolescent normal subjects and epilepsy patients were scanned using a 3 Tesla Magnetom Trio scanner (Siemens Medical Systems). Prior to study participation, subjects were familiarized with the MRI environment and sounds in a mock scanner, and then underwent a practice session with each of the behavioral tests. During scanning, foam padding was used to reduce motion artifacts, and improve subject comfort. Functional images were acquired with an echo-planar imaging (EPI) BOLD sequence (3.4 mm isotropic voxels, repetition time = 1550 ms, echo time = 30 ms, flip angle = 80°, matrix size = 64 × 64, 25 axial slices, thickness = 6 mm, field of view = 220 × 220 mm^2). At the beginning of each fMRI scan, a transistor–transistor logic pulse from the MRI scanner was used to initiate the visual stimulus presentation. Each fMRI run lasted 644.8 s, with a total of 416 volumes of data. Up to six (typically three or four) fMRI runs were obtained per recording session as tolerated by the subjects.

HCP gambling task data were collected on the 3 Tesla Siemens Connectome Skyra MRI scanner with a 32-channel head coil. All functional images were acquired using a multiband gradient-echo EPI imaging sequence (2 mm isotropic voxels, repetition time = 720 ms, echo time = 33.1 ms, flip angle = 52°, matrix size = 104 × 90, 72 axial slices, thickness = 2 mm, field of view = 208 × 180 mm^2). A total of 258 volumes were acquired per run for the gambling task, with two runs obtained per subject, each run lasting 192 s. Each subject underwent both the left-right (LR) and right-left (RL) phase-encoding data acquisition runs, and both were included in the analysis.

2.4. Preprocessing

For both the CPT/RTT and the HCP gambling task, standard pre-processing procedures were applied to the fMRI data. The SPM12 software package (http://www.fil.ion.ucl.ac.uk/SPM) was used for all fMRI pre-processing on a MATLAB platform. Subsequent analyses used SPM12 or custom scripts in MATLAB. The initial 10 volumes were discarded from each run of CPT/RTT data to allow for scanner stabilization. For the HCP data, 5 initial volumes were discarded automatically at the time of acquisition, so we discarded an additional 5 volumes, again yielding a total of 10 volumes discarded at the beginning of each run. The remaining images (406 frames for CPT/RTT and 248 frames for HCP gambling task) in each run were spatially realigned to the first image of each functional series, using 3D rigid body (linear) transformation with three translation and three rotation parameters. We required that the transient movement during a scanning run was no more than 1 mm of translation and 1° of rotation. 98 of 724 runs were discarded for the HCP gambling task, and 145 of 384 runs were discarded for CPT/RTT at this step (movement is more common in adolescents than in adults). Images were then spatially normalized to the SPM EPI template in MNI space and

smoothed using an isotropic Gaussian kernel. Smoothing kernel was 10 mm FWHM for CPT/RTT and 4 mm FWHM for HCP gambling task, selected to provide an effective smoothing FWHM at least twice the voxel size (3.4 mm for CPT/RTT and 2 mm for HCP gambling) (Friston et al., 1995). The standard 1/128 Hz high-pass filter from SPM was next applied to the data. Analyses were confined to cortical and subcortical gray matter voxels by using a standard gray matter mask from MARSBAR (http://marsbar.sourceforge.net/) and adding the predefined regions of midbrain and pons in xjview toolbox for SPM (www.alivelearn.net/xjview) by manually creating a template to include the gray matter in these structures based on a standard anatomical atlas (DeArmond et al., 1989). Our added gray matter template for midbrain and pons can be found at https://github.com/BlumenfeldLab/Rong-et-al_2020. The masking was implemented in first- and second- level statistical analyses using the explicit mask option in SPM, as well as in the percent change map and time course analyses.

Prior to further data analysis, signal-to-noise ratio (SNR) was calculated over time for each run [20*log (mean BOLD signal/standard deviation of BOLD signal)] then averaged over the whole brain. An arbitrary cut-off of 30 dB was set for exclusion, but all runs in the CPT/RTT and HCP gambling task exceeded the threshold, and none were discarded at this step.

2.5. fMRI statistical parametric mapping of transient and sustained effects

Our first goal was to examine the neural networks for transient fMRI changes occurring at the start of a block of task performance in different task paradigms and subject populations with a conventional HRF model analysis. In addition, we examined the sustained changes during task block performance. The transient responses were modeled by the standard SPM HRF placed at the task block onset and task block offset. The sustained response was modeled by convolving the canonical HRF with a boxcar of duration equal to the task block.

We first performed a general linear model (GLM) model analysis on the single-subject-level including all runs for each subject in SPM12. The model design matrix for each subject included a regressor for each run, transient and sustained regressors for CPT/RTT or the HCP gambling task, and six motion regressors obtained from the realignment step. Subsequently, first-level parameter estimates from the regressors of interest (task onset transient regressor, sustained regressor) were used for a group-level one-sample t-test across subjects in a second-level random-effects analysis. Statistical parametric maps for the task transient onset and sustained responses were computed for the CPT/RTT and the HCP gambling task. Of note, although the transient task offset signal was included as a regressor in the model along with the onset and sustained regressors, we only included onset and sustained maps in the figures, not offset maps, because of our interest in fMRI changes at task onset transitions. We used a family-wise error (FWE) corrected height threshold $p < 0.05$ to correct for multiple comparisons with an extent threshold of $k = 3$ voxels (voxel dimensions = $4 \times 4 \times 4$ mm) in all main analyses. In the smaller sample size ($n < 30$) subgroup analyses (Supplementary Figures) we included maps with a conservative but uncorrected height threshold $p < 0.005$ and an extent threshold of $k = 3$ to enable viewing of subthreshold changes, for comparison to the larger ($n > 30$) main analyses. Results were

displayed on the anatomical MRI template brain "colin27" (single_subj_T1 from SPM) in MNI space. Of note, identical methods were used for the CPT/RTT and the HCP gambling task data in our primary analyses of the block-design-related transient onset and sustained signals (see Fig. 1 and 2). In addition, because direct comparison of fMRI changes for the CPT task versus the RTT task showed no significant differences for the onset or sustained responses (at FWE $p < 0.05$; data not shown), we combined the CPT and RTT data sets for all analyses of block onset and sustained responses to increase sample size.

A possible concern with fMRI analysis methods is false-positive cluster detection (Eklund et al., 2016). Although FWE correction can lead to false-positive cluster detection, SPM (with cluster defining threshold $p = 0.001$, default) has much better FWE control than FSL (with cluster defining threshold $p = 0.01$, default), especially when implemented with larger voxel size ($4 \times 4 \times 4$ mm), and FWE correction is generally more conservative than false discovery rate (FDR) correction (Eklund et al., 2016). Nevertheless, to ensure that the clusters we identified in our data were not subject to cluster failure, we repeated our primary FWE-based analyses (shown in Figs. 1, 2) using Gaussian random field theory-based cluster-level correction for multiple comparisons, implemented in DPABI (http://rfmri.org/dpabi). As guided by previous work (Kessler et al., 2017), we used a cluster-defining voxel-level threshold of $p < 0.001$ and cluster-level $p < 0.05$ to evaluate the significance of corrected clusters. We found that this analysis, in fact, was less conservative and led to a larger number of significant regions (data not shown), which in all cases included the clusters found in our FWE-based analyses. We therefore chose to retain the more conservative FWE-corrected $p < 0.05$ results in our figures.

2.6. Voxel-based percent change map analysis

We next performed a model-free voxel-based analysis of fMRI percent signal changes over time for the whole brain as described previously (Bai et al., 2010; Guo et al., 2016) to examine the transient and sustained responses during the behavioral task blocks. Initial preprocessing and data exclusion criteria were the same as for the SPM analyses already described. In addition, instantaneous changes in head position, or framewise displacement (FD), were calculated as the sum of the absolute values of changes in the six parameters for transitional and rotational displacement between volumes (Power et al., 2012). The root mean squared (RMS) difference in BOLD signal from volume to volume was also calculated (referred to as DVARS). Volumes exceeding a DVARS threshold of 5 or an FD threshold of 0.3 were discarded as in previous studies (Power et al., 2012; Smyser et al., 2010), resulting in 11.0% of all volumes for CPT/RTT block time courses, 11.8% for event time courses and 1.6% of all volumes for HCP gambling task being discarded for percent change map calculations. Next, a standard GLM was used to regress out the effects of any remaining motion in the six directions (three translation, three rotation time courses determined in the realignment step). The time course of fMRI percent change was then calculated for each voxel as $100 \times (D1-D0)/D0$, where D1 was signal intensity over time and D0 was average signal intensity during the entire run. The fixation and task fMRI time periods were temporally aligned by task block onset, and mean time courses for each voxel were calculated across blocks in each run. To facilitate temporal alignment across runs, signals were interpolated from the acquisition time resolution (1.55 s for CPT/RTT and 0.72 s for

HCP gambling task) to 1 s intervals. In addition, to temporally align task onset and offset for CPT/RTT we included only data from 32 s task block runs (not 96 s task blocks), whereas for HCP gambling we included all runs. Finally, the mean block time course of each voxel was calculated by averaging across runs for each subject and then taking the mean across subjects. This resulted in a total of 1470 task blocks of fMRI data included in the averages for CPT/RTT, (10 blocks per run × total of 147 runs included from 46 subjects), and a total of 2504 task blocks for the HCP gambling task (4 blocks per run × total of 626 runs included from 336 subjects). Percent change maps were created for the entire brain at 1 s intervals using the resulting mean time courses, and again displayed on the anatomical MRI template brain "colin27" (single_subj_T1 from SPM) in MNI space. For visual inspection of these percent change maps, no statistical threshold was used in this analysis (see Fig. 3).

2.7. Mean time course analysis

A mean time course analysis was next performed in specific anatomical regions of interest (ROIs) using MARSBAR. The analysis used the same fMRI data as in the voxel-based percent change map analysis described above. As already noted in the previous section, to simplify temporal alignment of task onset and offset for CPT/RTT data we included only 32 s task block data (not 96 s task block data) in the fMRI percent change time course analyses. However, very similar results were obtained analyzing the CPT/RTT 96 s task blocks separately (data not shown). Four anatomic cortical and subcortical ROIs were selected based on known participation in the salience and arousal networks (Faingold and Blumenfeld, 2013; Kinomura et al., 1996; Schiff and Plum, 2000b; Van der Werf et al., 2002). Anterior insula/frontal operculum and supplementary motor area ROIs were constructed bilaterally from the standard MARSBAR regions (http://marsbar.sourceforge.net/) as follows: anterior insula/frontal operculum (Insula + Frontal_Inf_Oper + Frontal_Inf_Tri); supplementary motor area (Supp_Motor_Area). We constructed a spherical 7 mm radius ROI placed at the center of the midbrain gray matter tegmentum based on a standard atlas of human postmortem brain sections (DeArmond et al., 1989). For the thalamus we constructed an ROI spanning mainly intralaminar and medial thalamic regions known to be important for arousal and attention (Schiff, 2008; Schiff et al., 2013)(see Fig. 4 A). Thus for the thalamus ROI we used the Morel Atlas (Krauth et al., 2010; Morel et al., 1997) based on human postmortem histology to include the medial dorsal as well as thalamic intralaminar (central lateral, central medial, centromedian, parafascicular) nuclei (see Fig. 4 B). Our midbrain and thalamic ROIs are publicly available through https://github.com/BlumenfeldLab/Rong-et-al_2020. The time course of each ROI was analyzed by aligning data relative to task block onset. The mean time course was calculated by averaging fMRI data first across blocks for each run, next across runs for each subject, then across voxels within each anatomic ROI for each subject. Finally, means and statistics were calculated across subjects. To identify times with significant mean fMRI changes across subjects we performed a two-tailed t-test for each time point (1 s intervals) compared to 5 s baseline before task block onset with significance threshold $p < 0.05$, Bonferroni-corrected for number of time points.

2.8. Event-related analysis

To investigate the regions that were significantly involved in the processing of individual target event stimuli, we conducted an event-related analysis. For this analysis it was necessary to use only data in which the events were jittered in time, because when stimuli occur at regular, closely spaced intervals (fixed 1 s interval for the RTT task, fixed 3.5 s interval for the gambling task) the fMRI signals summate at steady-state, making event-related signals difficult to resolve. Therefore, we only used data from the CPT task, in which target stimuli were jittered at random intervals (average inter-target interval 4 s), for the event-related analysis ($n = 45$ subjects; one subject only had RTT runs). Even with the temporally-jittered data from the CPT task, the mean inter-target interval of 4 s was relatively short compared to other studies where target stimulus and block-related fMRI signals have been successfully modeled and separated (Chawla et al., 1999; Donaldson et al., 2001; Petersen and Dubis, 2012). Thus, as noted in the Results section, conventional event-related analysis yielded no significant activations for the CPT task.

A novel analysis method was therefore required for our more closely spaced stimuli in the CPT task (for code see https://github.com/BlumenfeldLab/Rong-et-al_2020). To detect signals related to individual stimuli closely spaced in time, it was necessary to effectively remove confounding signals-of-no-interest related to the block design. An important challenge in removing block-related signals is the fact that the time course of block-related signals varies substantially from region to region and is not uniformly well-described by the standard HRF model throughout the brain (Gonzalez-Castillo et al., 2012). Conventional HRF models incorrectly assume that the block-related fMRI time course has the same general shape for each voxel, modelled as a simple box car function convolved with a standard HRF. To overcome this, we calculated the mean block-related fMRI time course for each voxel in the brain across all blocks, and used this to remove the block-related nuisance signals in each individual subject. Of note, this mean fMRI time course across blocks *would* include the temporally consistent block-related signals, but would *not* include signals related to individual target stimuli. This is because the timing of individual targets varied randomly from block to block, and so their effect would be removed by the averaging across blocks. This is similar to standard artifact-removal approaches such as averaging and subtraction of gradient or ballistocar-diogram artifacts in EEG signals during fMRI acquisition (Allen et al., 2000; Goncalves et al., 2007) or regression of confounding signals in resting fMRI data (Fox et al., 2005c; Satterthwaite et al., 2013). Importantly, our regression of the block-related signals based on subject averages was not a circular pre-fit analysis, because it was used to remove signals-of-no-interest, and not to model the event-related signals being studied. To be sure this point is clear, we did not employ this novel voxel-by-voxel regression of the mean block-related signals in any analyses in which the blocks themselves represented signal of interest (e.g. Figs. 1 and 2; see above section, *fMRI statistical parametric mapping of transient and sustained effects*). We only applied this method to the event-related analysis (see Fig. 5), where block-related signals were considered as noise, or signals of no interest.

To perform this analysis, we again first performed a single-subject-level GLM analysis in SPM 12 including all runs for each subject. The model design matrix included event

regressors consisting of a standard HRF located after each target event, and the 6 motion regressors. In addition, to adequately account for the relatively large block-related fMRI signals which vary across location in the brain, we created separate block-related models for each voxel in the brain for each subject using their average fMRI percent change map time courses calculated as described above for each voxel. The block-related mean percent change time course for each voxel was aligned to the block timing and included as voxel-specific regressors in the design matrix for each run through an edited version of the spm_spm.m file (see https://github.com/BlumenfeldLab/Rong-et-al_2020). The parameter estimates obtained in this manner for each run were then averaged within sub- ject, and results from this first-level analysis were then entered into a second-level random-effects group analysis across subjects using a one sample t-test. We again corrected for multiple comparison with FWE-corrected height threshold $p < 0.05$, extent threshold of $k = 3$ voxels for our main analysis (see Fig. 5). As noted above, we also repeated analyses using Gaussian random field-based cluster-level multiple comparisons correction using the same method already described above for analysis of transient and sustained effects (Kessler et al., 2017), and after confirming that our results were not subject to cluster failure, retained the FWE-corrected results. In addition, as above for smaller sample size subgroup analyses we also viewed results using an uncorrected threshold of $p < 0.005$ (see Supplementary Figures 8 and 9). Mean fMRI time courses for all significant voxels were generated using the same averaging and statistics as in the ROI-based mean time course analyses already described for the block design, but using the overall run average as base-line.

To disambiguate between the transient signal related to attentional demand with the onset of a salient stimulus versus signal due to on-set of any visual stimulus, we replicated the above analysis using an event-related regressor that simply corresponded to randomly selected non-target stimuli, equal in number to the target stimuli. That is, we conducted a GLM analysis on the CPT task runs identical to above, but looking at the significance of a regressor consisting of a standard HRF at each randomly selected non-target stimulus. As in the analysis of the target stimuli, we looked at the maps using both an FWE-corrected threshold of $p < 0.05$ and uncorrected threshold of $p < 0.005$.

2.9. Conjunction analysis

To identify spatial and temporal similarities between 1) task onset transient, 2) sustained and 3) event-related signals with both tasks and subject groups, we performed conjunction analysis. We first identified all shared voxels for fMRI increases in both the transient and sustained t-maps, looking separately at the CPT/RTT and the HCP gambling data (see Figs. 1, 2). We constructed conjunction maps showing the spatial overlap between transient and sustained fMRI increases and then displayed the fMRI time courses in these regions using the methods described in the mean time course analysis section above. Next we performed an overall conjunction analysis combining the transient t-maps from the CPT/RTT and the HCP gambling task (see Fig. 1A and Fig. 2A) with the event-related fMRI increases from CPT (see Fig. 5). For these overall conjunction maps of transient task onset and event-related signals we then generated fMRI time courses for CPT/RTT block design, HCP gambling block design and CPT events, using the same averaging and statistics as in the ROI-based mean time course analyses already described (see Fig. 6).

2.10. Data and code availability statement

Data for the HCP gambling task are freely available in the public domain through the Human Connectome Project website as detailed in the Methods section. Data for the CPT/RTT task are available from the corresponding author subject to anonymization to protect privacy of clinical data and implementation of a data sharing agreement as required by the local IRB. Regions of interest for analyses are publicly available through MARSBAR or through https://github.com/BlumenfeldLab/Rong-et-al_2020 as described in the Methods. All codes for analyses in this study are publicly available through the SPM12 website as described in the Methods, combined with our add-on functions built in MATLAB and publicly available through https://github.com/BlumenfeldLab/Rong-et-al_2020. The above data and code sharing plans conform fully to the policies of our funding agencies and IRB.

3. Results

3.1. Transient pulse and sustained changes through fMRI statistical mapping

We first show the analysis of fMRI data from 46 adolescent subjects during the continuous performance task and repetitive tapping task (CPT/RTT) (Fig. 1). The analysis used a model including an onset-transient stick function, an offset-transient stick function, and a sustained boxcar function, each convolved with the standard HRF. We observed a significant (FWE-corrected $p < 0.05$) positive transient onset response at the start of the task block in the subcortical arousal systems including midbrain tegmentum (MT), thalamus (Th), nucleus basalis (NB) and striatum (Str); salience network regions including the anterior insula/claustrum (AI/C) and anterior cingulate cortex/supplementary motor area (AC/SMA); dorsal attention network regions including dorsolateral frontal cortex (DLF) and inferior parietal lobule (IPL); and motor regions including cerebellum (CB), and left hemisphere hand primary motor cortex (M1; button pushes were performed with the right hand) (Fig. 1A). Significant sustained increases were seen in regions of the Str, AI/C, AC/SMA, IPL, CB and M1, (Fig. 1B) also present in conjunction analysis of transient onset and sustained changes (Fig. 1C). The time course of fMRI changes in the conjunction analysis regions demonstrated a significant transient pulse increase at task block onset, as well as increases for part of the sustained period and task offset (Fig. 1D).

Of note, our initial exploratory analysis began with a smaller group of only normal adolescent subjects ($n = 22$). Due to smaller sample size, at FWE $p < 0.05$ this subgroup only showed increases in a subset of the regions described above for Fig. 1 (see Supplementary Figure 2A), however with less conservative uncorrected threshold $p < 0.005$ positive transient onset responses were seen in nearly identical regions of MT, Th, Str, AI/C, AC/SMA, DLF, CB and M1 as in Fig. 1 (see Supplementary Figure 2E). As we describe below and in the sections that follow, these changes were also consistently seen in a much larger cohort of normal subjects in the HCP data, as well as in event-related analysis of the CPT task. Therefore, to facilitate conjunction analysis using the same threshold across tasks and cohorts, and to increase sample size we included previously collected data from adolescent subjects with absence epilepsy in the CPT/RTT analysis, using only data with no seizures. The results from this second smaller cohort alone ($n = 24$) again showed significant increases in only a subset of the transient task block onset regions de- scribed above

(Supplementary Figure 3A), with the larger arousal and attention network only emerging with a less conservative uncorrected threshold (Supplementary Figure 3E). Of note, despite some differences in these maps, the arousal and attention network regions seen in subthreshold analyses of both the smaller normal cohort alone (Supplementary Figure 2E) and the epilepsy cohort alone (Supplementary Figure 3E) were highly overlapping as shown by conjunction analysis (Supplementary Figure 4). Therefore, to increase statistical power for analysis of transient onset changes we felt it was justified to combine these groups. In further support of this, the combined larger sample ($n = 46$) of CPT/RTT data showed significant (FWE $p < 0.05$) transient block on-set increases in the subcortical-cortical regions consistent with the other data sets discussed below, despite inclusion of both normal subjects and individuals with absence epilepsy (Fig. 1). Overall, these results with CPT/RTT data show a transient pulse of fMRI increases at task block onset involving subcortical and cortical arousal, salience and attention networks (MT, Th, Str, AI/C, AC/SMA, DLF, IPL), as well as motor (M1, CB) regions, followed by lower-amplitude increases in these regions during task blocks.

As we have just discussed, to further investigate the anatomically interesting transient fMRI changes observed with the CPT/RRT data, we performed the same analysis on a much larger data set ($n = 362$ subjects) of block-design data from normal adults in the Human Connectome Project (HCP) gambling task (Fig. 2). The results from the CPT/RTT data were further supported by the observation of anatomically similar transient onset maps in the gambling task. With the much larger data sample used for the HCP gambling task we again saw significant onset t-map increases at the start of the task block in the subcortical arousal systems and a set of functional regions including the MT, Th, Str, AI/C and AC/SMA as well as the DLF, IPL, CB and left M1 (Fig. 2A). Significant fMRI increases were also seen in these same regions in the sustained maps (Fig. 2B). In addition, the HCP gambling task more strongly activated the visual cortex (VCx) and deactivated the default mode regions including the ventral medial frontal cortex (VMPFC) and precuneus (PC) compared to CPT/RTT at the task onset and during the sustained period (Fig. 2A, B). Conjunction analysis demonstrated the overlapping regions of activation from the onset and sustained maps in the HCP gambling data (Fig. 2C, D). Thus, the results in this second larger cohort again demonstrate transient fMRI pulse increases at task onset in subcortical and cortical arousal, salience and attention networks, which in this case overlapped more strongly with subsequent increases during the sustained task blocks.

Previous work has demonstrated that the first trial of a block after a rest period often has significantly slower response times than other trials in the block; and autonomic or arousal-related effects may play a role during task reengagement (Barber et al., 2020, 2016; Poljac et al.,2009). In agreement with these concepts, we found that in all three types of task blocks, CPT, RTT and gambling, the first trial of a block had significantly longer response times than the remaining trials (all $p < 0.001$, two-tailed t-tests).

3.2. Data-driven analysis of task block onset: fMRI percent change maps

To examine transient fMRI changes at task block onset without a priori assumptions we next used a model-free approach of massive averaging (Gonzalez-Castillo et al., 2012; Guo et al.,

2016). We constructed maps of mean percent fMRI signal changes for the CPT/RTT and the HCP gambling task, averaged across all blocks, runs and subjects (Fig. 3). Here we do not statistically threshold the percent change maps but are showing a qualitative view of the spatial distribution of fMRI changes. Viewing the data in this way revealed a shared complex dynamic sequence of subcortical and cortical changes in response to onset of both tasks. Shortly after the CPT/RTT onset, fMRI increases were observed in subcortical regions including MT, Th, NB, Str, and also in cortical regions including the AI/C, AC/SMA, DLF and IPL. Negative fMRI responses occurred later in default mode network including the VMPFC and PC (Fig. 3A). Percent fMRI signal changes from only the 22 healthy normal adolescents and 24 epilepsy patients were also analyzed separately to eliminate possible disease-related effects, and these results showed very similar dynamic changes in subcortical and cortical regions (see Supplementary Figures 5 and 6).

Similarly, the HCP gambling task showed early fMRI increases in the MT, Th, NB, Str, AI/C, AC/SMA, and DLF. Subsequently, we again observed fMRI decreases in default mode VMPFC and PC, and also saw sustained fMRI increases in the VCx not observed in the CPT/RTT data (Fig. 3B). The complex dynamics of the fMRI changes over time including transient increases in additional subcortical arousal areas such as NB and cerebellum and in cortical regions such as the left hemisphere hand primary motor cortex can be more fully appreciated through the complete series of percent change maps (Supplementary PowerPoints 1, 2).

3.3. Mean time courses of transient task onset pulse responses in cortical-subcortical arousal systems

To further examine transient and sustained responses, we selected four anatomical ROIs in cortical (anterior insula/frontal operculum, supplementary motor cortex) and subcortical (MT, Th) regions based on their known functions in arousal and attention (Faingold and Blumenfeld, 2013; Kinomura et al., 1996; Schiff and Plum, 2000b; Van der Werf et al., 2002). fMRI time courses for all these regions in both tasks showed a significant positive transient onset response with initiation of task blocks (Fig. 4; see also Supplementary Figure 7 for the healthy normal adolescents and epileptic patients separately). The CPT/RTT time courses showed more prominent task offset transient activation com- pared to the gambling task, whereas the gambling task showed relatively larger sustained increases in fMRI signal during the task blocks. These results revealed a consistent involvement of subcortical arousal systems and certain cortical regions in the transient onset pulse responses in both CPT/RTT and HCP gambling task. Some different response patterns across task paradigms, including the larger offset transient responses in CPT/RTT and larger sustained fMRI increases during the gambling task blocks were also present. Of note, unlike CPT/RTT the gambling task had a substantial difference in visual input between the fixation and task blocks (see Methods), which may have led to stronger driving of visual cortex (e.g. Fig. 3B) and other areas during task blocks.

3.4. Event-related changes in cortical-subcortical networks

In addition to transient increases in attention at task block onset, we were also interested in transient increases in attention with the appearance of each target stimulus. Therefore, we

performed event-related analysis across individual targets. Events occurring at regular short intervals are not readily resolved with fMRI, however events jittered in time are well-suited for analysis (Huettel et al., 2014). Therefore, we limited our event-related analysis to the 45 subjects who performed the CPT task (Fig. 5; see also Supplementary Figure 8 for only healthy normal adolescents and Supplementary Figure 9 for only epilepsy patients), which had random interstimulus intervals. However, conventional analysis where the same block onset, offset and sustained regressors were used for all regions, and including regressors for individual target events (Chawla et al., 1999; Donaldson et al., 2001; Petersen and Dubis, 2012), did not yield any significant changes with event-related analysis (data not shown).

A novel analysis approach was needed to account for the fact that individual event-related signals are small compared to sustained task block-related fMRI changes, and the shape of block-related fMRI signals varies from region to region (e.g. see Fig. 4). As described in the Methods, we therefore used the mean block-related fMRI signal time courses for each voxel as regressors, to more effectively average and remove the anatomical variation in block-related fMRI signals, without removing the individual event-related signals in our event-related design. With this approach we observed transient fMRI increases with individual targets in the same cortical-subcortical arousal and attention networks seen previously for task block onset analyses, including MT, Th, Str, AI/C, AC/SMA and DLF (Fig. 5A; see also Supplementary Figure 8 for only healthy normal adolescents and Supplementary Figure 9 for only epilepsy patients). The mean fMRI time course of these events resembled the transient pulse increases observed after task block onset, peaking a few seconds after stimulus presentation (Fig. 5B). To distinguish signals associated with transient attention due to target stimuli vs. signals due to onset of any visual stimulus, we repeated the analysis using random target letters instead of the target letters as the events, and found no significant fMRI increases at either the standard or uncorrected threshold (data not shown). These findings suggest that task block onset and single trial events involve fMRI changes in similar cortical-subcortical arousal and attention networks, visualized through conjunction analysis in the next section.

Because an earlier positron emission tomography (PET) study showed a negative correlation between mean regional cerebral blood flow (rCBF) in cingulate cortex and mean reaction times (Naito et al., 2000), we correlated fMRI signal with reaction times on the CPT task (reaction times were not readily available for the other tasks). However, we found no significant correlation between reaction times and BOLD fMRI signals either for the overall BOLD response during CPT blocks or for individual CPT events, analyzed both using selective ROIs (including ACC) as well as the whole brain (data not shown).

3.5. Overall conjunction analysis of transient block onset and event-related signals

We performed an overall conjunction analysis to identify shared fMRI increases from 1. CPT/RTT and the HCP gambling task block onset, and 2. CPT event-related activity. This revealed a common network of cortical and subcortical regions including MT, Th, Str, AI/C, AC/SMA, DLF and left M1 involved in all conditions (Fig. 6A). Strikingly, this common shared network encompasses all major regions of the cortical and subcortical arousal, salience and attention networks.

We next examined the mean fMRI time courses for the conjunction analysis-based common shared network in the CPT event-related data, CPT/RTT block data and gambling block data (Fig. 6B). This revealed a similar transient initial peak in all three data sets, followed by sustained signals for the CPT/RTT and gambling block data which resembled the time courses obtained earlier (Fig. 1, 2, 5) with typical transient onset pulse responses in all conditions.

4. Discussion

We found a shared common network of subcortical and cortical regions participating in a transient pulse of fMRI increases at both task block onset and individual target events during cognitive tasks that require changes in attentional engagement. The network includes subcortical regions important in arousal such as midbrain tegmentum and thalamus including the intralaminar and medial thalamic nuclei, as well as cortical-subcortical networks for attentional salience and top-down control such as anterior insula/frontal operculum, claustrum, striatum, anterior cingulate/supplementary motor area and dorsolateral frontal cortex. The inferior parietal lobule and basal forebrain/nucleus basalis also appeared in some of the transient onset or sustained block-related analyses. Hand primary motor cortex, cerebellar and primary visual cortical activations appeared as expected for the button responses with right hand and visual stimuli in both the CPT/RTT and gambling task. Finally, the default mode network showed depressed activity during task blocks as previously demonstrated, which was more prominent in the task paradigm with stronger primary visual cortical activation. Results were consistent for both model-based GLM analyses, and for data-driven fMRI percent change maps based on massive signal averaging, and the common shared network regions were seen across the two different subject populations and task paradigms, as well as during transient task block onset, and event-related responses.

These findings support a model in which transitions in attention involve a widespread pulse in activity in subcortical and cortical arousal and attention networks that may dynamically modulate attentional state. Recent models of attentional control tend to emphasize cortical systems involved in top-down and bottom-up regulation of attention or internal versus externally-directed attention but do not address the potential role of coordinated subcortical and cortical activity in large-scale network switching (Corbetta and Shulman, 2002a; Fortenbaugh et al., 2017; Helfrich et al., 2019; Raichle and Snyder, 2007). Earlier theories of attention did include a potential enabling role for subcortical structures (Mesulam, 1981, 2000; Mohanty et al., 2008; Posner and Rothbart, 2007; Posner et al., 2006) but recent models focus mainly on the cortex and little work has addressed how dynamic changes in subcortical and cortical networks may participate in shifts of attention during tasks. Mixed block and event-related designs are very commonly used in cognitive neuroscience and involve abrupt externally-driven increases in attention with onset of blocks and individual task stimuli, as well as sustained top-down increases in endogenous attention during task blocks. These important transitions in attention are true for well-known tasks of attentional vigilance such as the CPT used here, and even in tasks not designed specifically to study attention, such as the gambling task used in the Human Connectome Project. Although prior studies have reported elements of the cortical and subcortical networks described here, they

did not focus on common regions associated with transient block onset and target event-related activity across task paradigms. This was achieved in our study due to use of relatively large sample sizes heightening the ability to detect subcortical changes in small structures together with combined analyses of diverse subject populations and tasks. This approach allowed us to elucidate the shared neural substrates of transient changes in attention particularly in subcortical arousal structures, and the dynamic time course of these changes which may be crucial for driving neural systems between attention states. It is interesting that the fMRI signals we observed, particularly in subcortical arousal structures showed a transient timecourse, more prominently rising and falling than expected from known hemodynamic effects alone for a sustained box car function, unless transient neural activity were superimposed (Fig. 4 A, B; Fig. 6). Of course it is important to emphasize that fMRI measurements may not directly reflect neural activity of the regions imaged, and additional direct electrophysiological studies of the subcortical arousal structures are needed in human subjects or animal models, as discussed further below.

Although other studies have not demonstrated the complete set of subcortical-cortical regions with the consistency that we have shown here across conditions, components of the network have been studied extensively in previous work shedding light on their functions (Satpute et al., 2019). The subcortical task onset responses in MT and Th in our results are in agreement with an earlier positron emission tomography study demonstrating increased cerebral blood flow in these regions during a reaction-time task (Kinomura et al., 1996). The upper brainstem tegmentum regions showing increases in the present study encompass multiple parallel neurotransmitter systems involved in arousal, including midbrain and upper pontine reticular formation, pedunculopontine and laterodorsal tegmental nuclei, parabrachial nuclei, dorsal and median raphe, locus coeruleus and periaqueductal gray matter extending to the pretectal area and posterior hypothalamus (Blumenfeld, 2015; Motelow and Blumenfeld, 2014). Interesting recent studies have demonstrated the potentially important role of transient changes in subcortical-cortical cholinergic neuromodulation in attentional target detection (Howe et al., 2013; Lu et al., 2020; Parikh and Sarter, 2008; Sarter and Lustig, 2019, 2020). Previous studies have also demonstrated that the transient response of intralaminar thalamus is linked to intensive orienting and alerting stimuli (Sanford et al., 1992a, 1992b). The intralaminar thalamus receives extensive monosynaptic input from the mesencephalic reticular formation and in turn projects to many cortical regions (Moruzzi and Magoun, 1949; Steriade and Glenn, 1982). Thus MT and Th are key components of the ascending arousal systems that modulate shifts of attentional vigilance (Edlow et al., 2012; Li et al., 2019; Nagai et al., 2004; Schiff and Plum, 2000a; Van der Werf et al., 2002; Yanaka et al., 2010). The striatum (Li et al., 2018; Schiff, 2008; Schiff et al., 2013), and nucleus basalis (Fuller et al., 2011; Raver and Lin, 2015) are also thought to participate in these circuits. The claustrum is further postulated to participate in widespread cortical integration, attention and consciousness (Crick and Koch, 2005). fMRI studies often identify the anterior insula/frontal operculum as key components of the salience network. Because the fMRI signals in reality overlap both insula and claustrum we have included the claustrum, designating this region as "AI/C". In sum, diverse subcortical regions implicated in arousal, attention and consciousness contribute to the transient pulse of fMRI increases we observed in the present study. Although the function of this pulse is

unknown, we can speculate that it may involve a neuromodulatory surge in multiple parallel neurotransmitter systems facilitating dynamic changes in conscious attention.

Cortical regions in our conjunction analysis have been implicated previously in externally oriented attention, event detection, conscious visual perception and motor preparation (Barcelo, 2003; Barry et al., 2012; Corbetta and Shulman, 2002b; Menon and Uddin, 2010; Nagai et al., 2004) as well as in the salience network (Menon and Uddin, 2010; Seeley et al., 2007) and ventral attention system (Corbetta and Shulman, 2002b; Kincade et al., 2005). It is well established that the AI and AC/SMA are hubs of the salience network or ventral attention system that detect unattended or unexpected stimuli, triggering shifts of attention (Astafiev et al., 2003; Nagai et al., 2004; Seeley et al., 2007; Vossel et al., 2014). These same regions are active at the initiation or termination of tasks (Dosenbach et al., 2008, 2007, 2006; Fox et al., 2005a; Konishi et al., 2001; Paret et al., 2014). Another cortical region showing positive responses at block transitions is the SMA, implicated in motor preparation during orientation and attention (Lee et al., 1999), onset and offset of responses to stimuli associated with the contingent negative variation (Nagai et al., 2004). It is interesting that although a prior PET study showed a negative correlation between mean reaction times and mean rCBF in the anterior cingulate (Naito et al., 2000), we did not find significant relationships between reaction times and event or block-related BOLD fMRI changes. It is likely that differences in temporal resolution, measured signal (CBF versus BOLD) or other experimental factors may account for these different findings. Notably, in agreement with previous work (Barber et al., 2020, 2016; Poljac et al., 2009), we found that the first trial of a block in our tasks had slower reaction time than the remaining trials, an observation previously associated with autonomic or arousal-related effects during task reengagement. The possible relation of the subcortical-cortical networks described here to reaction times or other behavioral parameters should be investigated further in future work.

The spatial relationship between transient and sustained fMRI responses has been examined in previous work (Dosenbach et al., 2008, 2007, 2006; Fox et al., 2005a, 2005b; Uludag, 2008), as well as topographical differences between transient responses at task block onset and offset. It is important to point out that the CPT task is a true attentional vigilance task, with the RTT and the HCP gambling requiring progressively less attentional vigilance. The different tasks require different amounts of attentional engagement, and the cognitive processes involved in a target stimulus in the CPT task is not the same as initiating the task block. However, these conditions are similar in that they all require shifts from a state of vigilant anticipation to active stimulus detection and engagement, either beginning from rest or from an already heightened state of attention during task blocks. The transient pulse of subcortical and cortical increases we observed in common shared arousal, salience and top-down attentional networks may thus be related to the initiation of these shifts occurring from different baseline states.

Once the task has been initiated, heightened attention is sustained throughout the subsequent task block. The mechanisms for transitioning brain networks from block initiation to maintenance are not known, however the initial pulse may be similar to other biological or mechanical systems where initial viscosity or resistance to change is overcome by a large pulse of activity driving the system into a new state (pulse-step model) (Ghez and Vicario,

1978; Karniel and Inbar, 1999; Schor and Bharadwaj, 2006; Sparks and Mays, 1990; Wallen and Astrom, 2002). Notably, we observed sustained fMRI increases to some extent in the same networks where the pulse occurred, however the sustained increases were much more variable between anatomical regions and tasks. For example, the sustained increases in attention/arousal networks were larger in gambling than in the CPT/RTT task (Fig. 1, 2 and 4). This may appear paradoxical, because the CPT/RTT tasks would generally be considered more attentionally demanding than the gambling task. However, other differences between the tasks or populations could account for the larger sustained fMRI increases in the gambling task. First of all, the task- related fMRI increases in primary visual cortex were substantially larger for the HCP gambling task (Figs. 2–3) than for CPT/RTT (Fig. 1). This was likely because visual stimuli in the gambling task were not matched in color, contrast or luminance to the fixation cross, unlike the CPT/RTT task where task and fixation stimuli were carefully matched. It is also possible that the distinct developmental stages of two populations and different cognitive mechanisms underlying the CPT/RTT and HCP gambling task might contribute to these different BOLD responses in VCx. It is also important to note that because the stimuli during blocks were closely spaced in time in our paradigms, the sustained fMRI changes we observed during blocks include activity related to both sustained attention and repeated task stimuli during the blocks. Therefore, signals related to repeated stimuli during blocks might also contribute to differences in sustained fMRI signals between CPT/RTT and the gambling task blocks, separately from any differences in sustained attention with these tasks. Second, in addition to the larger sustained increases in attention/arousal networks in the gambling task, there were also larger decreases in the default mode network compared to in the CPT/RTT task. Previous fMRI studies have demonstrated that stronger default mode network deactivation is associated with greater activation of visual cortical excitability (Greicius and Menon, 2004; Mo et al., 2013). Therefore, it is possible that the stronger sustained changes may also have been driven by stronger VCx activation in the gambling task blocks compared to CPT/RTT, although again it is possible that other mechanisms could contribute. The cause for somewhat different magnitudes in the timecourse of changes in different anatomical regions (e.g. Fig. 4) is unknown but might be related to varying hemodynamic and neural factors between these areas. Finally, it should also be noted that the transient fMRI increases at the end of task blocks was larger for CPT/RTT than for gambling. Offset transients have been observed previously in task-based fMRI studies (e.g. (Gonzalez-Castillo et al., 2012; Konishi et al., 2001)) and it is unclear why this was less prominent in the gambling HCP data. However, we can speculate that this might be related to task differences and different BOLD responses in different regions, including the fact that in the gambling task (unlike CPT/RTT) the fixation cross appears intermittently within task blocks as well as during fixation, so it is less novel when it appears at the end of the task block. In addition, as already noted the gambling task elicited larger sustained fMRI increases which could make transient increases at task block end more difficult to see.

To increase sample size, we included data from epilepsy patients along with normal adolescents in our analyses of CPT and RTT, taking care to use only data runs with no epileptiform activity on EEG recorded simultaneously. We observed that results generated using normal subjects alone were not substantially changed by adding the patients with

epilepsy, except that the increased sample size strengthened the significance of the observed fMRI changes (please compare Supplementary Figure 2E vs. Fig. 1A; Supplementary Figure 5 vs. Fig. 3A; Supplementary Figure 8C vs. Fig. 5; see also Supplementary Figure 7 for direct comparison of epilepsy vs. normal fMRI timecourses). Nevertheless, we acknowledge that patients with epilepsy may have deficits in attention (Killory et al., 2011; Vega et al., 2010) which should be investigated further in relation to fMRI change in future studies. In addition, although we observed similar transient fMRI changes in subcortical and cortical networks in several cohorts and tasks in the present work, it will be important to expand these investigations to other tasks and groups to determine if the observed transient network changes are more broadly seen. It is interesting that very similar transient fMRI changes were observed in the midbrain, thalamus, striatum and multiple cortical regions with task block onset and target events, in two different tasks, in adolescents and in adults, in normal subjects and people with epilepsy. Future studies should include additional tasks, and larger groups of normal subjects as well as subjects with different disorders to further determine the consistency of this subcortical-cortical network in health and in disease.

The fMRI findings reported here of transient activity increases in cortical and subcortical arousal systems are supported by prior direct electrophysiological studies in humans and animal models (Nagai et al., 2004; Raver and Lin, 2015; Sanford et al., 1992a, 1992b; Schiff et al., 2013; Van der Werf et al., 2002). An advantage of fMRI is that it provides an assessment of transient changes throughout the human brain with comprehensive anatomical sampling in cortical and subcortical structures not available with more spatially limited electrophysiological methods. However, fMRI is indeed limited in its temporal resolution to the order of seconds. Further investigation of the sub-second temporal relationships between subcortical and cortical signals and the neural mechanisms of the observed transient fMRI changes could be investigated in animal models through direct electrophysiological recordings, or potentially in future human studies with increasing availability of subcortical depth electrodes used for therapeutic interventions (Fisher et al., 2010; Kronemer et al., 2017; Velasco et al., 2007). Another interesting avenue for future research would be the possible role of arousal and autonomic mechanism in attention transitions (Barber et al., 2020, 2016; Poljac et al., 2009), which could be pursued by relating the slower response times we observed in the initial trial of each block to autonomic measurements and fMRI changes.

In summary, the current study has identified a common shared network of dynamic transient fMRI increases in subcortical arousal structures and in a set of cortical functional regions during performance of attention-demanding behavioral tasks. We consistently observed a transient pulse of fMRI increases at task block onset in the subcortical MT, Th and Str, as well as regions belonging to salience and attention networks including AI/C, AC/SMA and DLF regardless of population and task paradigm differences. Importantly, event-related analysis of individual target stimuli showed similar activations in the same subcortical-cortical networks. The striking shared participation of subcortical and cortical arousal, salience and attention networks in these transient changes support a model in which a large pulse of activity in these systems acts cooperatively to initiate and maintain changes in attention.

Supplementary Material

Refer to Web version on PubMed Central for supplementary material.

Acknowledgments

References

Allen PJ, Josephs O, Turner R, 2000. A method for removing imaging artifact from continuous EEG recorded during functional MRI. Neuroimage 12, 230–239. [PubMed: 10913328]

Astafiev SV, Shulman GL, Stanley CM, Snyder AZ, Van Essen DC, Corbetta M, 2003. Functional organization of human intraparietal and frontal cortex for attending, looking, and pointing. J. Neurosci 23, 4689–4699. [PubMed: 12805308]

Bai X, Guo J, Killory B, Vestal M, Berman R, Negishi M, Danielson N, Novotny EJ, Constable RT, Blumenfeld H, 2011. Resting functional connectivity between the hemispheres in childhood absence epilepsy. Neurology 76, 1960–1967. [PubMed: 21646622]

Bai X, Vestal M, Berman R, Negishi M, Spann M, Vega C, Desalvo M, Novotny EJ, Constable RT, Blumenfeld H, 2010. Dynamic time course of typical childhood absence seizures: EEG, behavior, and functional magnetic resonance imaging. J. Neurosci 30, 5884–5893. [PubMed: 20427649]

Barber AD, John M, DeRosse P, Birnbaum ML, Lencz T, Malhotra AK, 2020. Parasympathetic arousal-related cortical activity is associated with attention during cognitive task performance. Neuroimage 208, 116469.

Barber AD, Pekar JJ, Mostofsky SH, 2016. Reaction time-related activity reflecting periodic, task-specific cognitive control. Behav. Brain Res 296, 100–108. [PubMed: 26318935]

Barcelo F, 2003. The Madrid card sorting test (MCST): a task switching paradigm to study executive attention with event-related potentials. Brain. Res. Brain Res. Protoc 11, 27–37. [PubMed: 12697260]

Barch DM, Burgess GC, Harms MP, Petersen SE, Schlaggar BL, Corbetta M, Glasser MF, Curtiss S, Dixit S, Feldt C, Nolan D, Bryant E, Hartley T, Footer O, Bjork JM, Poldrack R, Smith S, Johansen-Berg H, Snyder AZ, Van Essen DC, Consortium WU-MH, 2013. Function in the human connectome: task-fMRI and individual differences in behavior. Neuroimage 80, 169–189. [PubMed: 23684877]

Barry RJ, Steiner GZ, De Blasio FM, 2012. Event-related EEG time-frequency analysis and the Orienting Reflex to auditory stimuli. Psychophysiology 49, 744–755. [PubMed: 22524168]

Blumenfeld H, 2015. Neuroanatomical Basis of Consciousness. In: The Neurology of Consciousness, 2nd Edition. Eds: Gosseries O, Laureys S, Tononi G. Elsevier, Ltd. Ch 1.

Buckner RL, Bandettini PA, O'Craven KM, Savoy RL, Petersen SE, Raichle ME, Rosen BR, 1996. Detection of cortical activation during averaged single trials of a cognitive task using functional magnetic resonance imaging. Proc. Natl. Acad. Sci. U. S. A 93, 14878–14883. [PubMed: 8962149]

Cauda F, Costa T, Diano M, Sacco K, Duca S, Geminiani G, Torta DM, 2014. Massive modulation of brain areas after mechanical pain stimulation: a time-resolved FMRI study. Cereb. Cortex 24, 2991–3005. [PubMed: 23796948]

Chawla D, Rees G, Friston KJ, 1999. The physiological basis of attentional modulation in extrastriate visual areas. Nat. Neurosci 2, 671–676. [PubMed: 10404202]

Corbetta M, Shulman GL, 2002a. Control of goal-directed and stimulus-driven attention in the brain. Nat. Rev. Neurosci 3, 201–215. [PubMed: 11994752]

Corbetta M, Shulman GL, 2002b. Control of goal-directed and stimulus-driven attention in the brain. Nat. Rev. Neurosci 3, 201–215. [PubMed: 11994752]

Crick FC, Koch C, 2005. What is the function of the claustrum? Philoso. Trans. R. Soc. London - Ser. B: Biol. Sci 360, 1271–1279.

DeArmond SJ, Fusco MM, Dewey MM, 1989. Structure of the Human brain: a Photographic Atlas, 3rd ed. Oxford University Press, New York.

Delgado MR, Nystrom LE, Fissell C, Noll DC, Fiez JA, 2000. Tracking the hemodynamic responses to reward and punishment in the striatum. J. Neurophysiol 84, 3072–3077. [PubMed: 11110834]

Donaldson DI, Petersen SE, Ollinger JM, Buckner RL, 2001. Dissociating state and item components of recognition memory using fMRI. Neuroimage 13, 129–142. [PubMed: 11133316]

Dosenbach NU, Fair DA, Cohen AL, Schlaggar BL, Petersen SE, 2008. A dual-networks architecture of top-down control. Trends Cogn. Sci 12, 99–105. [PubMed: 18262825]

Dosenbach NU, Fair DA, Miezin FM, Cohen AL, Wenger KK, Dosenbach RA, Fox MD, Snyder AZ, Vincent JL, Raichle ME, Schlaggar BL, Petersen SE, 2007. Distinct brain networks for adaptive and stable task control in humans. PNAS 104, 11073–11078. [PubMed: 17576922]

Dosenbach NU, Visscher KM, Palmer ED, Miezin FM, Wenger KK, Kang HC, Burgund ED, Grimes AL, Schlaggar BL, Petersen SE, 2006. A core system for the implementation of task sets. Neuron 50, 799–812. [PubMed: 16731517]

Edlow BL, Takahashi E, Wu O, Benner T, Dai G, Bu L, Grant PE, Greer DM, Greenberg SM, Kinney HC, Folkerth RD, 2012. Neuroanatomic connectivity of the human ascending arousal system critical to consciousness and its disorders. J. Neuropathol. Exp. Neurol 71, 531–546. [PubMed: 22592840]

Eklund A, Nichols TE, Knutsson H, 2016. Cluster failure: why fMRI inferences for spatial extent have inflated false-positive rates. Proc. Natl. Acad. Sci. U. S. A 113, 7900–7905. [PubMed: 27357684]

Faingold C, Blumenfeld H, 2013. Neuronal networks in brain function, CNS disorders, and Therapeutics. Academic Press.

Fisher R, Salanova V, Witt T, Worth R, Henry T, Gross R, Oommen K, Osorio I, Nazzaro J, Labar D, Kaplitt M, Sperling M, Sandok E, Neal J, Handforth A, Stern J, DeSalles A, Chung S, Shetter A, Bergen D, Bakay R, Henderson J, French J, Baltuch G, Rosenfeld W, Youkilis A, Marks W, Garcia P, Barbaro N, Fountain N, Bazil C, Goodman R, McKhann G, Babu Krishnamurthy K, Papavassiliou S, Epstein C, Pollard J, Tonder L, Grebin J, Coffey R, Graves N, Group SS, 2010. Electrical stimulation of the anterior nucleus of thalamus for treatment of refractory epilepsy. Epilepsia 51, 899–90. [PubMed: 20331461]

Fortenbaugh FC, DeGutis J, Esterman M, 2017. Recent theoretical, neural, and clinical advances in sustained attention research. Ann. N. Y. Acad. Sci 1396, 70–91. [PubMed: 28260249]

Fox MD, Snyder AZ, Barch DM, Gusnard DA, Raichle ME, 2005a. Transient BOLD responses at block transitions. Neuroimage 28, 956–966. [PubMed: 16043368]

Fox MD, Snyder AZ, McAvoy MP, Barch DM, Raichle ME, 2005b. The BOLD onset transient: identification of novel functional differences in schizophrenia. Neuroimage 25, 771–782. [PubMed: 15808978]

Fox MD, Snyder AZ, Vincent JL, Corbetta M, Van Essen DC, Raichle ME, 2005c. The human brain is intrinsically organized into dynamic, anticorrelated functional networks. PNAS 102, 9673–9678. [PubMed: 15976020]

Friston KJ, Holmes AP, Poline JB, Grasby PJ, Williams SC, Frackowiak RS, Turner R, 1995. Analysis of fMRI time-series revisited. Neuroimage 2, 45–53. [PubMed: 9343589]

Fuller PM, Sherman D, Pedersen NP, Saper CB, Lu J, 2011. Reassessment of the structural basis of the ascending arousal system. J. Comp. Neurol 519, 933–956. [PubMed: 21280045]

Ghez C, Vicario D, 1978. The control of rapid limb movement in the cat. II. Scaling of isometric force adjustments. Exp. Brain Res 33, 191–202. [PubMed: 700005]

Goncalves SI, Pouwels PJ, Kuijer JP, Heethaar RM, de Munck JC, 2007. Artifact removal in co-registered EEG/fMRI by selective average subtraction. Clin. Neurophysiol 118, 2437–2450. [PubMed: 17889599]

Gonzalez-Castillo J, Saad ZS, Handwerker DA, Inati SJ, Brenowitz N, Bandettini PA, 2012. Whole-brain, time-locked activation with simple tasks revealed using massive averaging and model-free analysis. PNAS 109, 5487–5492. [PubMed: 22431587]

Greicius MD, Menon V, 2004. Default-mode activity during a passive sensory task: uncoupled from deactivation but impacting activation. J. Cogn. Neurosci 16, 1484–1492. [PubMed: 15601513]

Guo JN, Kim R, Chen Y, Negishi M, Jhun S, Weiss S, Ryu JH, Bai X, Xiao W, Feeney E, Rodriguez-Fernandez J, Mistry H, Crunelli V, Crowley MJ, Mayes LC, Constable RT, Blumenfeld H, 2016. Impaired consciousness in patients with absence seizures investigated by functional MRI, EEG, and behavioural measures: a cross-sectional study. Lancet Neurol. 15, 1336–1345. [PubMed: 27839650]

Helfrich RF, Breska A, Knight RT, 2019. Neural entrainment and network resonance in support of top-down guided attention. Curr. Opin. Psychol 29, 82–89. [PubMed: 30690228]

Hodge MR, Horton W, Brown T, Herrick R, Olsen T, Hileman ME, McKay M, Archie KA, Cler E, Harms MP, Burgess GC, Glasser MF, Elam JS, Curtiss SW, Barch DM, Oostenveld R, Larson-Prior LJ, Ugurbil K, Van Essen DC, Marcus DS, 2016. ConnectomeDB–Sharing human brain connectivity data. Neuroimage 124, 1102–1107. [PubMed: 25934470]

Howe WM, Berry AS, Francois J, Gilmour G, Carp JM, Tricklebank M, Lustig C, Sarter M, 2013. Prefrontal cholinergic mechanisms instigating shifts from monitoring for cues to cue-guided performance: converging electrochemical and fMRI evidence from rats and humans. J. Neurosci 33, 8742–8752. [PubMed: 23678117]

Huettel SA, Song AW, McCarthy G, 2014. Functional Magnetic Resonance Imaging, 3rd Edition Sinauer Associates, Inc. Sunderland, MA.

Karniel A, Inbar GF, 1999. The Use of a Nonlinear Muscle Model in Explaining the Relationship Between Duration, Amplitude, and Peak Velocity of Human Rapid Movements. J. Mot. Behav 31, 203–206. [PubMed: 11177631]

Kessler D, Angstadt M, Sripada CS, 2017. Reevaluating "cluster failure" in fMRI using nonparametric control of the false discovery rate. Proc. Natl. Acad. Sci 114, E3372–E3373. [PubMed: 28420796]

Killory BD, Bai X, Negishi M, Vega C, Spann MN, Vestal M, Guo J, Berman R, Danielson N, Trejo J, Shisler D, Novotny EJ Jr., Constable RT, Blumenfeld H, 2011. Impaired attention and network connectivity in childhood absence epilepsy. Neuroimage 56, 2209–2217. [PubMed: 21421063]

Kincade JM, Abrams RA, Astafiev SV, Shulman GL, Corbetta M, 2005. An even-t-related functional magnetic resonance imaging study of voluntary and stimulus–driven orienting of attention. J. Neurosci 25, 4593–4604. [PubMed: 15872107]

Kinomura S, Larsson J, Gulyas B, Roland PE, 1996. Activation by attention of the human reticular formation and thalamic intralaminar nuclei. Science 271, 512. [PubMed: 8560267]

Konishi S, Donaldson DI, Buckner RL, 2001. Transient activation during block transition. Neuroimage 13, 364–374. [PubMed: 11162276]

Krauth A, Blanc R, Poveda A, Jeanmonod D, Morel A, Szekely G, 2010. A mean three-dimensional atlas of the human thalamus: generation from multiple histological data. Neuroimage 49, 2053–2062. [PubMed: 19853042]

Kronemer SI, Forman S, Ryu J, Khosla M, Sarberski E, Xiao WR, Constable R, Blumenfeld H, 2017. The cortical and subcortical neural mechanisms of visual perception. Soc. Neurosci. Abstracts. 2017 Abstract No. 804.12 Online at http://www.sfn.org/annual-meeting/past-and-future-annual-meetings.

Laureys S, Gosseries O, Tononi G, 2015. The Neurology of Consciousness: Cognitive Neuroscience and Neuropathology, 2nd Edition Academic Press.

Lee K–M, Chang K–H, Roh J–K, 1999. Subregions within the supplementary motor area activated at different stages of movement preparation and execution. Neuroimage 9, 117–123. [PubMed: 9918733]

Li R, Hu C, Wang L, Liu D, Liu D, Liao W, Xiao B, Chen H, Feng L, 2019. Disruption of functional connectivity among subcortical arousal system and cortical networks in temporal lobe epilepsy. Brain Imaging Behav. 1–10. [PubMed: 28466439]

Li R, Liao W, Yu Y, Chen H, Guo X, Tang YL, Chen H, 2018. Differential patterns of dynamic functional connectivity variability of striato-cortical circuitry in children with benign epilepsy with centrotemporal spikes. Hum. Brain Mapp 39, 1207–1217. [PubMed: 29206330]

Lu Y, Sarter M, Zochowski M, Booth V, 2020. Phasic cholinergic signaling promotes emergence of local gamma rhythms in excitatory-inhibitory networks. Eur. J. Neurosci 52, 3545–3560. [PubMed: 32293081]

May JC, Delgado MR, Dahl RE, Stenger VA, Ryan ND, Fiez JA, Carter CS, 2004. Event-related functional magnetic resonance imaging of reward-related brain circuitry in children and adolescents. Biol. Psychiatry 55, 359–366. [PubMed: 14960288]

Menon V, Uddin LQ, 2010. Saliency, switching, attention and control: a network model of insula function. Brain Struct. Funct 214, 655–667. [PubMed: 20512370]

Mesulam MM, 1981. A cortical network for directed attention and unilateral neglect. Ann. Neurol 10, 309–325. [PubMed: 7032417]

Mesulam MM, 2000. Principles of Behavioral and Cognitive Neurology, 2nd ed. Oxford University Press, Oxford; New York.

Mirsky AF, Vanburen JM, 1965. On the Nature of the "Absence" in Centrencephalic Epilepsy: a Study of Some Behavioral, Electroencephalographic and Autonomic Factors. Electroencephalogr. Clin. Neurophysiol 18, 334–348.

Mo J, Liu Y, Huang H, Ding M, 2013. Coupling between visual alpha oscillations and default mode activity. Neuroimage 68, 112–118. [PubMed: 23228510]

Mohanty A, Gitelman DR, Small DM, Mesulam MM, 2008. The spatial attention network interacts with limbic and monoaminergic systems to modulate motivation-in-duced attention shifts. Cereb. Cortex 18, 2604–2613. [PubMed: 18308706]

Morel A, Magnin M, Jeanmonod D, 1997. Multiarchitectonic and stereotactic atlas of the human thalamus. J. Comp. Neurol 387, 588–630. [PubMed: 9373015]

Moruzzi G, Magoun HW, 1949. Brain stem reticular formation and activation of the EEG. Electroencephalogr. Clin. Neurophysiol 1, 455–473. [PubMed: 18421835]

Motelow J, Blumenfeld H, 2014. Consciousness and Subcortical Arousal Systems. In: Faingold CL, Blumenfeld H (Eds), Neuronal Networks in Brain Function, CNS Disorders, and Therapeutics, Elsevier Ch 21, p. 277–298.

Nagai Y, Critchley HD, Featherstone E, Fenwick PB, Trimble MR, Dolan RJ, 2004. Brain activity relating to the contingent negative variation: an fMRI investigation. Neuroimage 21, 1232–1241. [PubMed: 15050551]

Naito E, Kinomura S, Geyer S, Kawashima R, Roland PE, Zilles K, 2000. Fast reaction to different sensory modalities activates common fields in the motor areas, but the anterior cingulate cortex is involved in the speed of reaction. J. Neurophysiol 83, 1701–1709. [PubMed: 10712490]

Paret C, Kluetsch R, Ruf M, Demirakca T, Kalisch R, Schmahl C, Ende G, 2014. Transient and sustained BOLD signal time courses affect the detection of emotion-related brain activation in fMRI. Neuroimage 103, 522–532. [PubMed: 25204866]

Parikh V, Sarter M, 2008. Cholinergic mediation of attention: contributions of phasic and tonic increases in prefrontal cholinergic activity. Ann. N. Y. Acad. Sci 1129, 225–235 [PubMed: 18591483]

Petersen SE, Dubis JW, 2012. The mixed block/event-related design. Neuroimage 62, 1177–1184. [PubMed: 22008373]

Poljac E, Koch I, Bekkering H, 2009. Dissociating restart cost and mixing cost in task switching. Psychol. Res 73, 407–416. [PubMed: 18446364]

Portas CM, Rees G, Howseman AM, Josephs O, Turner R, Frith CD, 1998. A specific role for the thalamus in mediating the interaction of attention and arousal in humans. J. Neurosci 18, 8979–8989. [PubMed: 9787003]

Posner JB, Saper CB, Schiff ND, Plum F, 2007. Plum and Posner's Diagnosis of Stupor and Coma, 4th ed. Oxford University Press, USA.

Posner MI, Rothbart MK, 2007. Research on attention networks as a model for the integration of psychological science. Annu. Rev. Psychol 58, 1–23. [PubMed: 17029565]

Posner MI, Sheese BE, Odludas Y, Tang Y, 2006. Analyzing and shaping human attentional networks. Neural Netw. 19, 1422–1429. [PubMed: 17059879]

Power J, KA B, AZ S, BL S, SE P, 2012. Spurious but systematic correlations in functional connectivity MRI networks arise from subject motion. Neuroimage 59, 2142–2154. [PubMed: 22019881]

Raichle ME, Snyder AZ, 2007. A default mode of brain function: a brief history of an evolving idea. Neuroimage 37, 1083–1090. [PubMed: 17719799]

Raver SM, Lin SC, 2015. Basal forebrain motivational salience signal enhances cortical processing and decision speed. Front. Behav. Neurosci 9, 277. [PubMed: 26528157]

Sanford LD, Ball WA, Morrison AR, Ross RJ, Mann G, 1992a. Peripheral and central components of alerting: habituation of acoustic startle, orienting responses, and elicited waveforms. Behav. Neurosci 106, 112–120. [PubMed: 1554425]

Sanford LD, Morrison AR, Ball WA, Ross RJ, Mann GL, 1992b. Varying expressions of alerting mechanisms in wakefulness and across sleep states. Electroencephalogr. Clin. Neurophysiol 82, 458–468. [PubMed: 1375554]

Sarter M, Lustig C, 2019. Cholinergic double duty: cue detection and attentional control. Curr. Opin. Psychol 29, 102–107. [PubMed: 30711909]

Sarter M, Lustig C, 2020. Forebrain cholinergic signaling: wired and phasic, not tonic, and causing behavior. J. Neurosci 40, 712–719. [PubMed: 31969489]

Satpute AB, Kragel PA, Barrett LF, Wager TD, Bianciardi M, 2019. Deconstructing arousal into wakeful, autonomic and affective varieties. Neurosci. Lett 693, 19–28. [PubMed: 29378297]

Satterthwaite TD, Elliott MA, Gerraty RT, Ruparel K, Loughead J, Calkins ME, Eickhoff SB, Hakonarson H, Gur RC, Gur RE, Wolf DH, 2013. An improved framework for confound regression and filtering for control of motion artifact in the preprocessing of resting-state functional connectivity data. Neuroimage 64, 240–256. [PubMed: 22926292]

Schiff ND, 2008. Central thalamic contributions to arousal regulation and neurological disorders of consciousness. Ann. N. Y. Acad. Sci 1129, 105–118. [PubMed: 18591473]

Schiff ND, Plum F, 2000a. The role of arousal and "gating" systems in the neurology of impaired consciousness. J. Clin. Neurophysiol 17, 438–452. [PubMed: 11085547]

Schiff ND, Plum F, 2000b. The role of arousal and "gating" systems in the neurology of impaired consciousness. J. Clin. Neurophysiol 17, 438–452. [PubMed: 11085547]

Schiff ND, Shah SA, Hudson AE, Nauvel T, Kalik SF, Purpura KP, 2013. Gating of attentional effort through the central thalamus. J. Neurophysiol 109, 1152–1163. [PubMed: 23221415]

Schor CM, Bharadwaj SR, 2006. Pulse-step models of control strategies for dynamic ocular accommodation and disaccommodation. Vision Res. 46, 242–258. [PubMed: 16289198]

Seeley WW, Menon V, Schatzberg AF, Keller J, Glover GH, Kenna H, Reiss AL, Greicius MD, 2007. Dissociable intrinsic connectivity networks for salience process- ing and executive control. J. Neurosci 27, 2349–2356. [PubMed: 17329432]

Shulman GL, Fiez JA, Corbetta M, Buckner RL, Miezin FM, Raichle ME, Petersen SE, 1997. Common blood flow changes across visual tasks: II. Decreases in cerebral cortex. J. Cogn. Neurosci 9 (5), 648–663. [PubMed: 23965122]

Smyser C, Inder T, Shimony J, Hill J, Degnan A, Snyder A, Neil J, 2010. Longitudinal analysis of neural network development in preterm infants. Cereb. Cortex 20, 2852–2862. [PubMed: 20237243]

Sparks DL, Mays LE, 1990. Signal transformations required for the generation of saccadic eye movements. Annu. Rev. Neurosci 13, 309–336. [PubMed: 2183679]

Steriade M, Glenn LL, 1982. Neocortical and caudate projections of intralaminar thalamic neurons and their synaptic excitation from midbrain reticular core. J. Neurophysiol 48, 352–371. [PubMed: 6288887]

Steriade MM, McCarley RW, 2010. Brain Control of Wakefulness and Sleep, 2nd ed Springer.

Tricomi EM, Delgado MR, Fiez JA, 2004. Modulation of caudate activity by action contingency. Neuron 41, 281–292. [PubMed: 14741108]

Uludag K, 2008. Transient and sustained BOLD responses to sustained visual stimulation. Magn. Reson. Imaging 26, 863–869. [PubMed: 18479869]

Van der Werf YD, Witter MP, Groenewegen HJ, 2002. The intralaminar and midline nuclei of the thalamus. Anatomical and functional evidence for participation in processes of arousal and awareness. Brain Res. Brain Res. Rev 39, 107–140. [PubMed: 12423763]

Van Essen DC, Smith SM, Barch DM, Behrens TE, Yacoub E, Ugurbil K, 2013. The WU-Minn Human Connectome Project: an overview. Neuroimage 80, 62–79. [PubMed: 23684880]

Vega C, Vestal M, DeSalvo M, Berman R, Chung M, Blumenfeld H, Spann MN, 2010. Differentiation of attention-related problems in childhood absence epilepsy. Epilepsy Behav. 19, 82–85 [NIHMS# 230291]. [PubMed: 20674507]

Velasco F, Velasco AL, Velasco M, Jimenez F, Carrillo-Ruiz JD, Castro G, 2007. Deep brain stimulation for treatment of the epilepsies: the centromedian thalamic target. Acta Neurochirurg. - Suppl 97, 337–342.

Visscher KM, Miezin FM, Kelly JE, Buckner RL, Donaldson DI, McAvoy MP, Bhalodia VM, Petersen SE, 2003. Mixed blocked/event-related designs separate transient and sustained activity in fMRI. Neuroimage 19, 1694–1708. [PubMed: 12948724]

Vossel S, Geng JJ, Fink GR, 2014. Dorsal and ventral attention systems: distinct neural circuits but collaborative roles. Neuroscientist 20, 150–159. [PubMed: 23835449]

Wallen A, Astrom KJ, 2002. Pulse-step control. IFAC Proc. Vol. 35, 175–180.

Yanaka HT, Saito DN, Uchiyama Y, Sadato N, 2010. Neural substrates of phasic alertness: a functional magnetic resonance imaging study. Neurosci. Res 68, 51–58. [PubMed: 20561955]
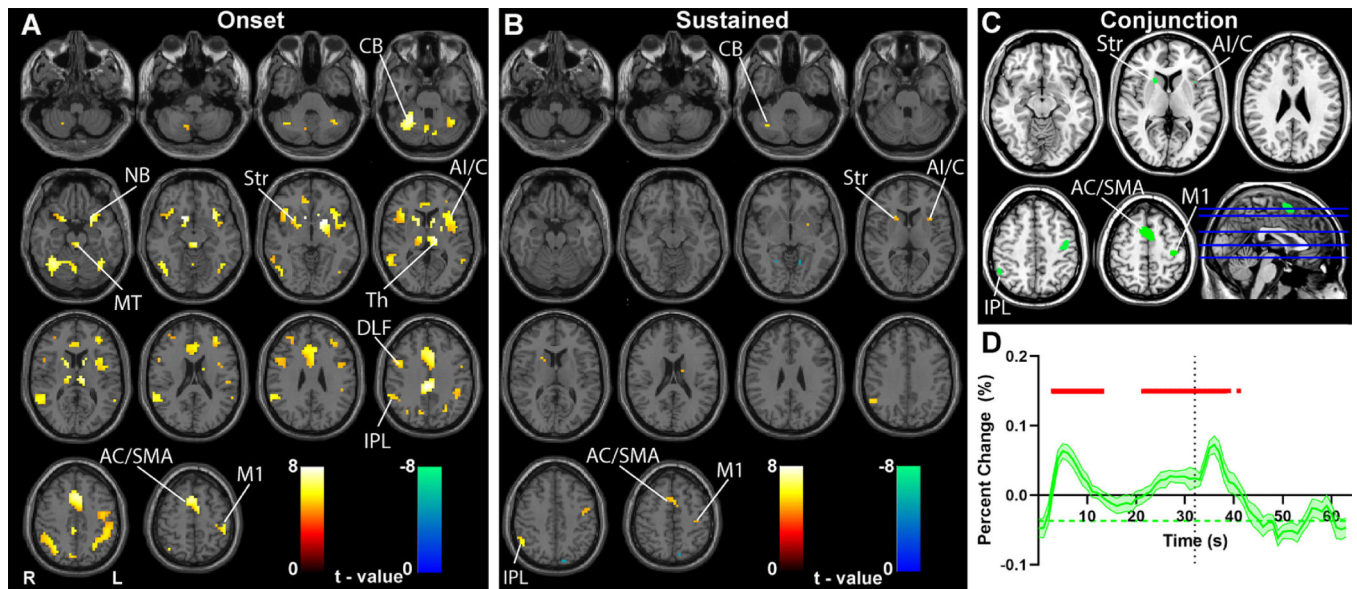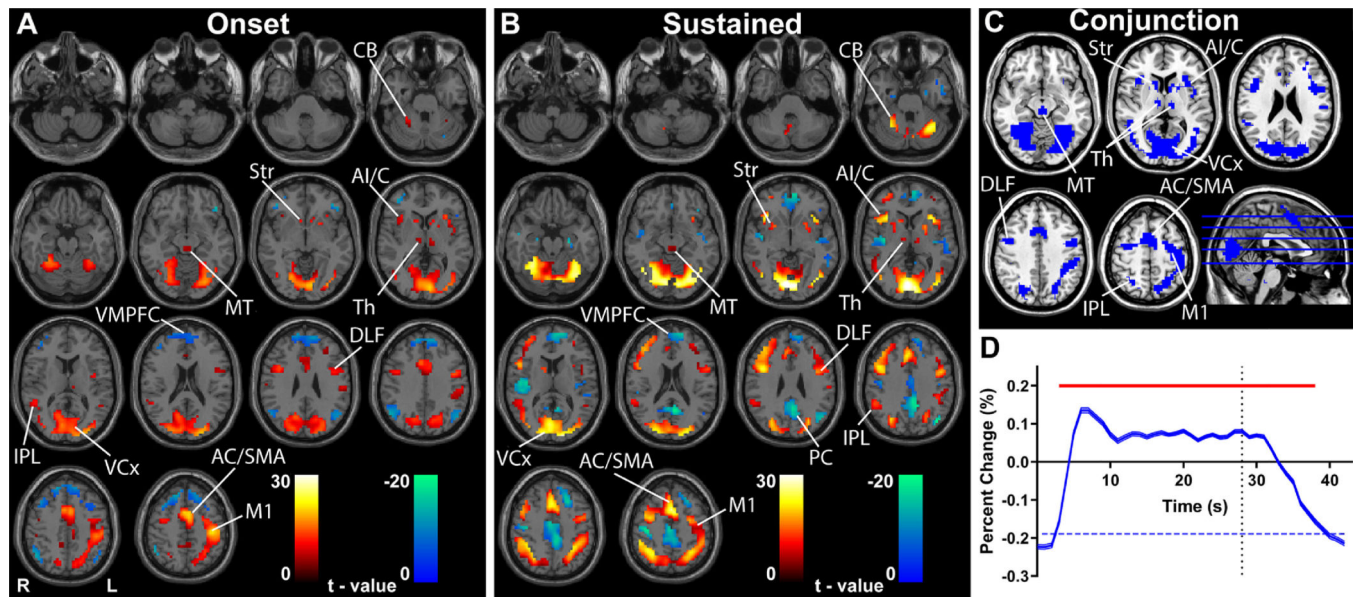
Fig. 1. Transient and sustained fMRI changes in subcortical and cortical networks during CPT/RTT task.

(A-B) GLM-based t-maps are shown for the transient onset HRF (A), and sustained boxcar function convolved with the HRF (B) at FWE-corrected height threshold $p < 0.05$ and extent threshold $k = 3$ voxels. (C) Conjunction analysis of fMRI increases in the onset and sustained t-maps from A and B. (D) Mean time course and standard error (across participants) of fMRI percent change in all voxels from conjunction analysis in C. For D, time 0 s is onset of CPT/RTT task block, and time 32 s is onset of fixation (indicated by vertical dotted line). Significant changes from baseline (horizontal green dashed line) are indicated by the horizontal red bars (two-tailed t-test, Bonferroni-corrected $p < 0.05$). Note that time courses in D show only the 32 s task block data to simplify temporal alignment of task onset and offset, however very similar results were obtained when analyzing the 96 s task blocks separately (data not shown). Warm colors in A and B show fMRI changes in parallel to the model and cool colors show negative changes. Midbrain tegmentum (MT), thalamus (Th), striatum (Str), nucleus basalis (NB), cerebellum (CB), anterior insula/claustrum (AI/C), inferior parietal lobule (IPL), anterior cingulate cortex (AC), supplementary motor area (SMA), dorsolateral frontal cortex (DLF), left hemisphere hand primary motor cortex (M1). $n = 46$ subjects.

Fig. 2. Transient and sustained fMRI changes in subcortical and cortical networks during the HCP gambling task.

(A-B) GLM-based t-maps for the transient onset HRF (A) and sustained boxcar function convolved with the HRF (B) at FWE-corrected height threshold $p < 0.05$ and extent threshold $k = 3$ voxels. Warm colors indicate fMRI changes in parallel to the model and cool colors show negative changes. (C) Conjunction analysis of fMRI increases in the onset and sustained t-maps from A and B. (D) Mean time course and standard error (across participants) of fMRI percent change in all voxels from conjunction analysis in C. Time 0 s is onset of HCP gambling task block, and time 28 s is onset of fixation (indicated by vertical dotted line). Significant changes from baseline (horizontal blue dashed line) are indicated by the horizontal red bar (two-tailed t-test, Bonferroni-corrected $p < 0.05$). Midbrain tegmentum (MT), thalamus (Th), striatum (Str), cerebellum (CB), anterior insula/claustrum (AI/C), inferior parietal lobule (IPL), anterior cingulate cortex (AC), supplementary motor area (SMA), dorsolateral frontal cortex (DLF), left hemisphere hand primary motor cortex (M1), ventral medial prefrontal cortex (VMPFC), precuneus (PC), visual cortex (VCx). $n = 362$ subjects.
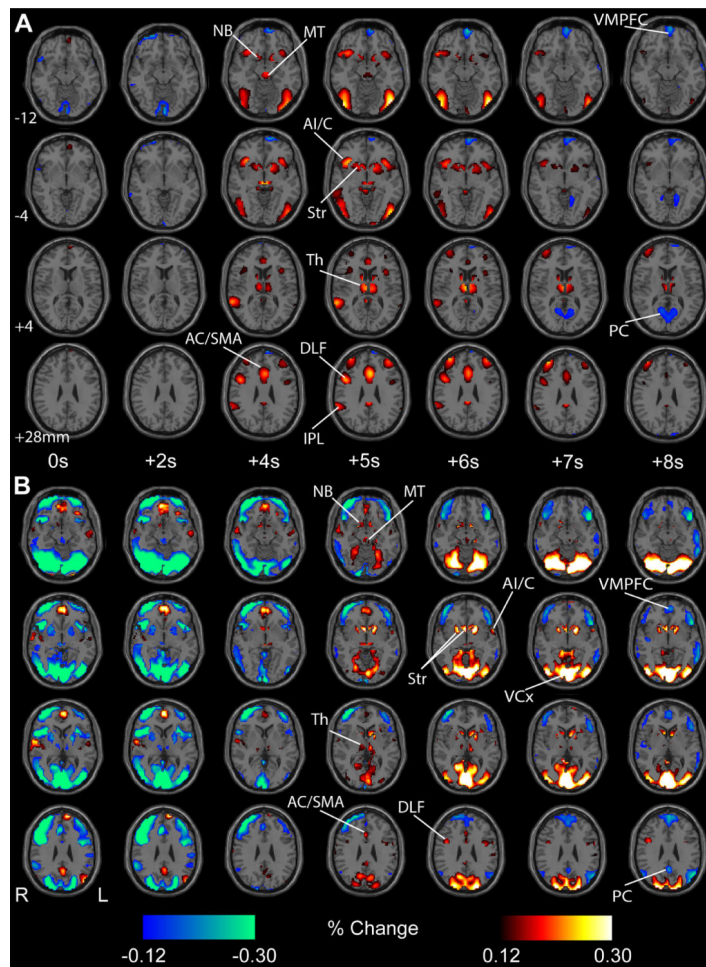
Fig. 3. Mean percent fMRI signal changes with task onset in 46 adolescents during the CPT/RTT task (A) and in 362 healthy adults during the gambling task (B).

fMRI percent change increases (warm colors) and decreases (cool colors) with respect to voxel baselines (whole run average) are shown, with a display threshold of 0.12%. Initial changes are shown for both tasks after block onset at 0 s. For both tasks, fMRI increases were observed in subcortical structures, including the midbrain tegmentum (MT), thalamus (Th), nucleus basalis (NB), and the striatum (Str), as well as in cortical regions, such as the such as the anterior insula/claustrum (AI/C), inferior parietal lobule (IPL), anterior cingulate cortex (AC), supplementary motor area (SMA) and dorsolateral frontal cortex (DLF). Later fMRI decreases occurred for both tasks in ventral medial frontal cortex (VMPFC) and precuneus (PC), and sustained increases were observed in visual cortex (VCx) with onset of the gambling task. Here we show only the 32 s task block data to simplify temporal alignment but very similar results were obtained analyzing the 96 s task blocks separately (not shown). No statistical threshold was used in this analysis. More detailed percent change maps for all time points and more brain slices can be seen in can be seen in Supplementary PowerPoint 1 for the CPT/RTT task, and Supplementary PowerPoint 2 for the gambling task. $n = 46$ subjects for CPT/RTT and $n = 362$ subjects for HCP gambling task.
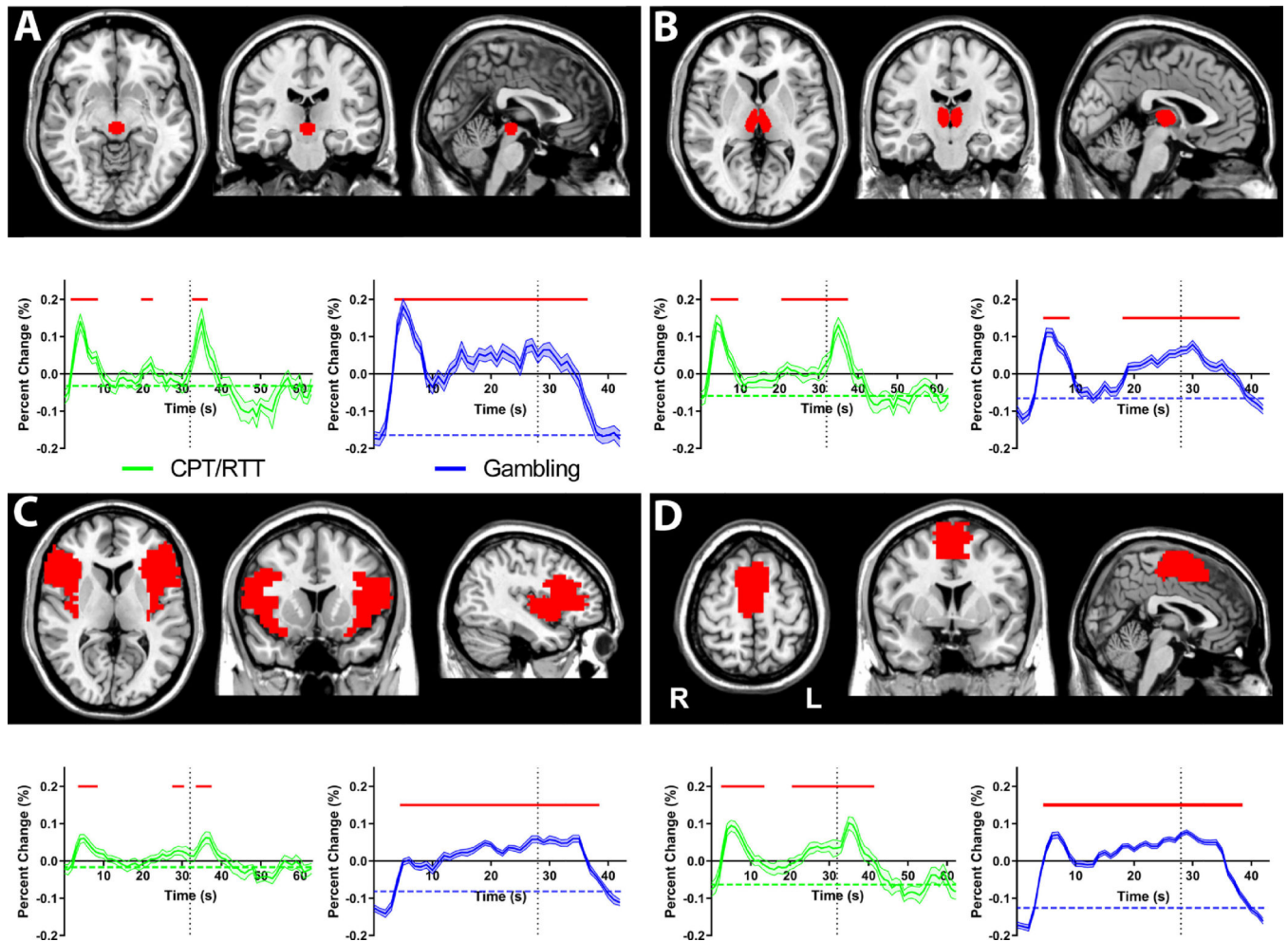
Fig. 4. Mean time courses of selected regions of interest showing transient onset responses for CPT/RTT and gambling task.

(A) midbrain tegmentum (B)thalamus (C) anterior insula/frontal operculum (D) supplementary motor area. The CPT/RTT time courses (green) are shown from 0 s to 63 s relative to the task onset, with task offset at 32 s (vertical dotted lines). The gambling task time courses (blue) are shown from 0 s to 42 s relative to the task onset, with task offset at 28 s. All time courses are mean and standard error across subjects, with significant changes from baseline (horizontal dashed lines) indicated by horizontal red bars (two-tailed t-test, Bonferroni-corrected $p < 0.05$). Same subjects and data as Fig. 3. Again, very similar results were obtained analyzing the 96 s CPT/RTT task blocks separately (data not shown).
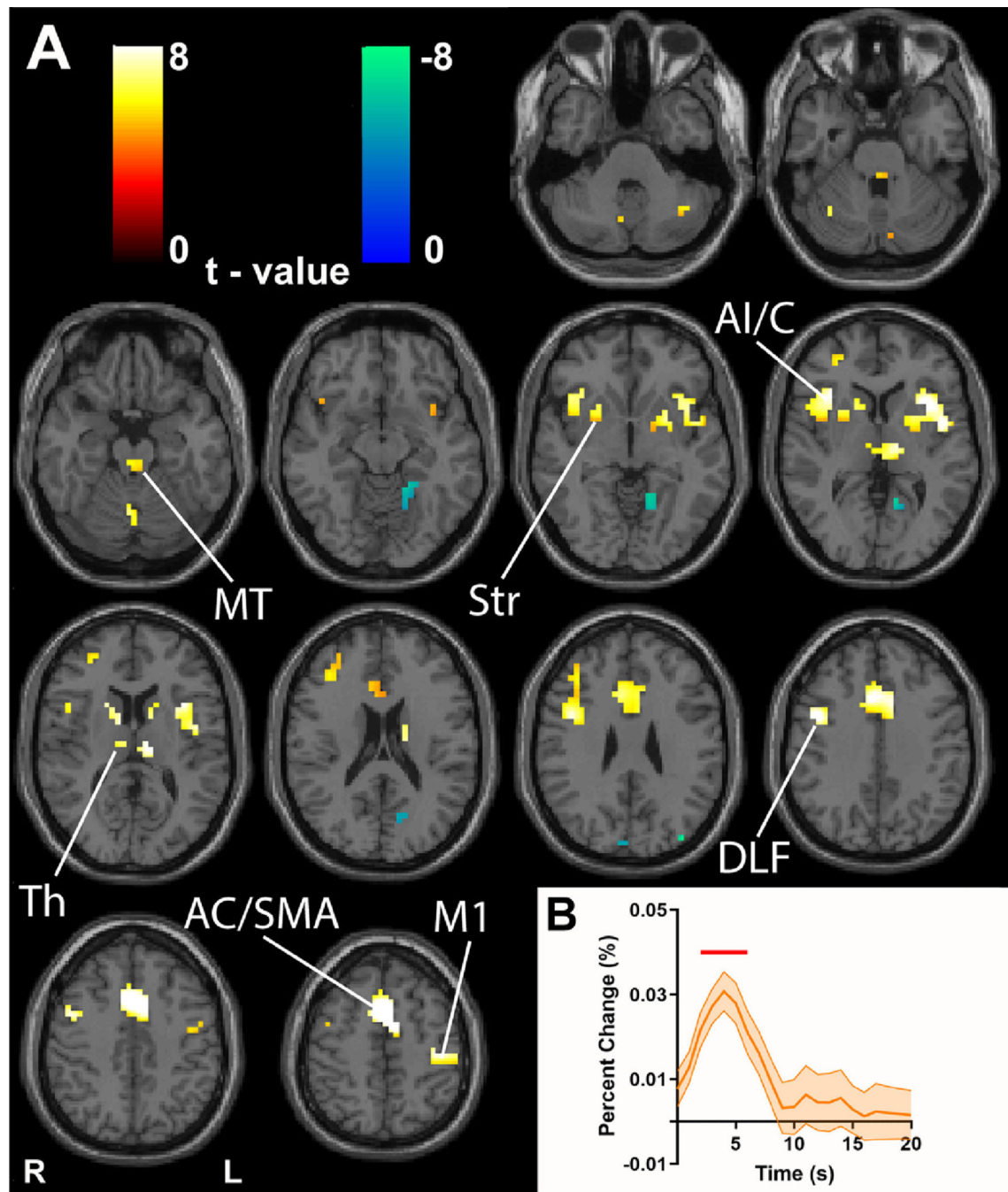
Fig. 5. Event-related analysis of individual CPT target stimuli reveals networks resembling transient task block onset activity.

(A) GLM-based t-maps illustrate event-related activity with extent threshold of $k = 3$ voxels and height thresholds of FWE-corrected $p < 0.05$. (B) fMRI mean time courses and standard error (across subjects) averaged across all voxels showing significant positive changes in t-map from A. Time points showing significant changes from baseline (two-tailed t-test, Bonferroni-corrected $p < 0.05$) are indicated by the horizontal red bar. Time 0 s is event onset for target stimuli. Midbrain tegmentum (MT), thalamus (Th), striatum (Str), anterior insula/claustrum (AI/C), anterior cingulate/supplementary motor area (AC/SMA),
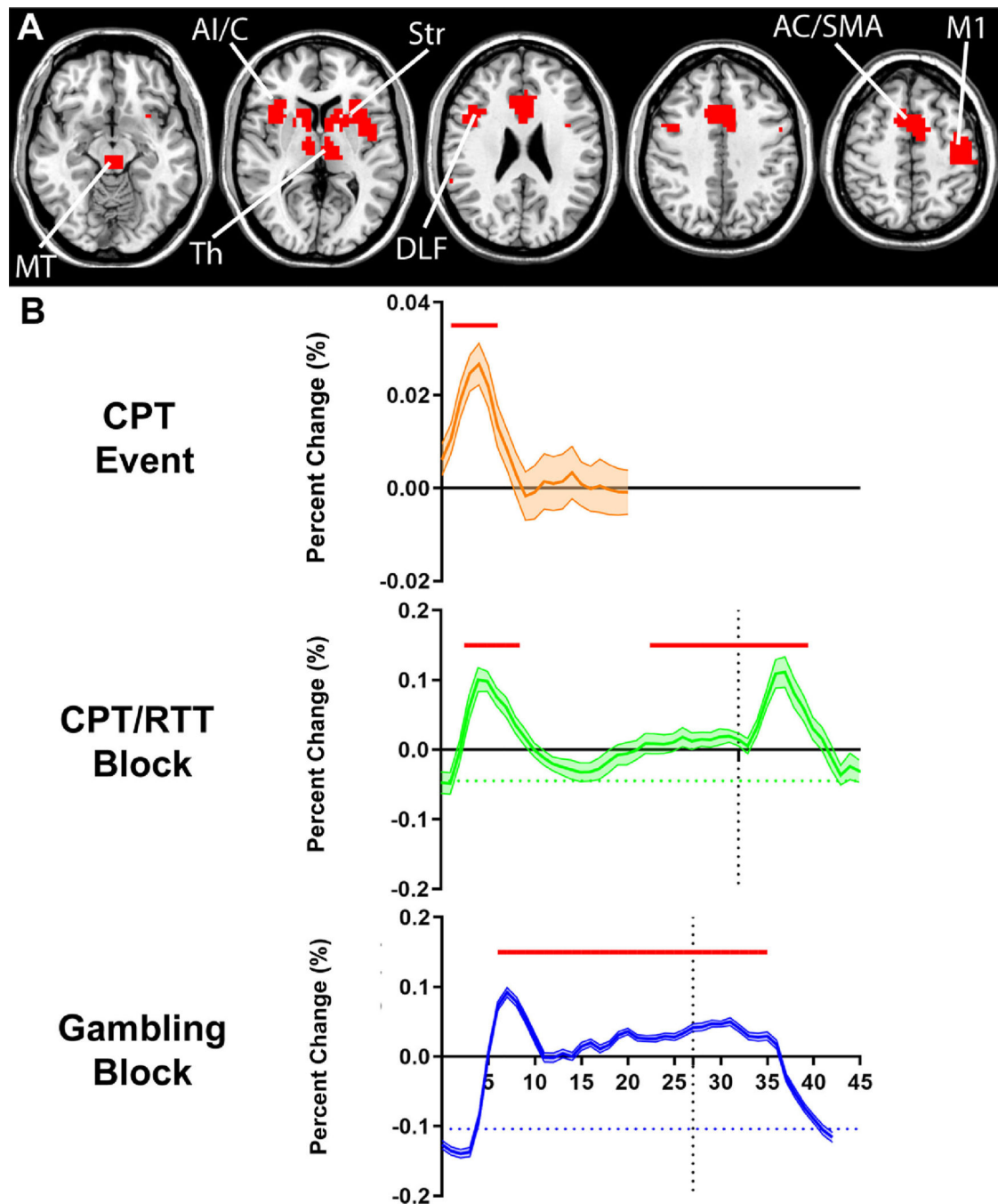
dorsolateral frontal cortex (DLF), left hemisphere hand primary motor cortex (M1). Warm colors indicate fMRI changes in parallel to the model and cool colors show negative changes. $n = 45$ subjects.

Fig. 6. Overall conjunction analysis of onset and event-related fMRI increases.
(A) Intersection of suprathreshold fMRI increases from the CPT/RTT onset analysis (Fig. 1A), HCP gambling onset analysis (Fig. 2A) and the CPT event-related analysis (Fig. 5A). Consistent activations in the midbrain tegmentum (MT), thalamus (Th), striatum (Str), anterior insula/claustrum (AI/C), anterior cingulate/supplementary motor area (AC/SMA), dorsolateral frontal cortex (DLF) and left hemisphere hand primary motor cortex (M1) were observed in the overlapped map across onset responses and the event-related responses. (B) Mean time courses of the regions in (A) for CPT event-related data, CPT/RTT task block

data, and the HCP gambling task block data. The time course is shown from 0 s to 20 s relative to the CPT event onset, 0 s to 63 s relative to the CPT/RTT task block onset, with task block offset at 32 s (vertical dotted line) and from 0 s to 42 s relative to the HCP gambling task block onset, with task block offset at 28 s (vertical dotted line). All time courses are mean and standard error across subjects, with significant changes from baseline (horizontal dashed lines) indicated by horizontal red bars (two-tailed t-test, Bonferroni-corrected $p < 0.05$). Data and subjects are same as in Figs. 1, 2 and 5.

Table 1

Subject demographics, summary of task conditions and scanner parameters.

Dataset	Yale adolescent subjects	Human connectome project
Number of subjects (females)	46 (20)	362 (186)
Mean subject age, years (range)	13 (11–19)	28 (22–35) [1]
Tasks	CPT, RTT	Gambling
Task blocks/run	10 or 5	4
Task block duration	32 s or 96 s	28 s
Fixation blocks/run	10 or 5	4
Fixation block duration	32 s	15 s
Task stimuli	Letters [2]	Colored symbols [2]
Target stimulus duration	250 ms	Up to 1.5 s
Target stimulus ITI	4 s average for CPT, 1 s for RTT [3]	3.5 s
Behavioral response	R hand button response	R hand button response
Resting stimulus	Fixation cross	Fixation cross
Scanner	Siemens, 3 T	Siemens, 3 T
BOLD TR	1.55 s	720 ms
BOLD TE	30 ms	33.1 ms

CPT = continuous performance task; RTT = repetitive tapping task; ITI = inter-trial interval.

[1] Of the 362 subjects, 359 were between the ages of 22–35, 3 were older than 36.

[2] Letters in CPT task had same average contrast and luminance as fixation cross. Colored symbols and other stimuli in gambling task were not matched to the fixation cross.

[3] The stimulus ITI for CPT varied randomly between trials with an average ITI of 4 s.